Published in final edited form as:
Prog Biophys Mol Biol. 2007 ; 93(1-3): 212–255.

Ultrasound—biophysics mechanisms†

William D. O'Brien Jr.*
Bioacoustics Research Laboratory, Department of Electrical and Computer Engineering, University of Illinois, 405 N. Mathews, Urbana, IL 61801, USA

Abstract

Ultrasonic biophysics is the study of mechanisms responsible for how ultrasound and biological materials interact. Ultrasound-induced bioeffect or risk studies focus on issues related to the effects of ultrasound on biological materials. On the other hand, when biological materials affect the ultrasonic wave, this can be viewed as the basis for diagnostic ultrasound. Thus, an understanding of the interaction of ultrasound with tissue provides the scientific basis for image production and risk assessment. Relative to the bioeffect or risk studies, that is, the biophysical mechanisms by which ultrasound affects biological materials, ultrasound-induced bioeffects are generally separated into thermal and nonthermal mechanisms. Ultrasonic dosimetry is concerned with the quantitative determination of ultrasonic energy interaction with biological materials.

Whenever ultrasonic energy is propagated into an attenuating material such as tissue, the amplitude of the wave decreases with distance. This attenuation is due to either absorption or scattering. Absorption is a mechanism that represents that portion of ultrasonic wave that is converted into heat, and scattering can be thought of as that portion of the wave, which changes direction. Because the medium can absorb energy to produce heat, a temperature rise may occur as long as the rate of heat production is greater than the rate of heat removal. Current interest with thermally mediated ultrasound-induced bioeffects has focused on the thermal isoeffect concept. The non-thermal mechanism that has received the most attention is acoustically generated cavitation wherein ultrasonic energy by cavitation bubbles is concentrated. Acoustic cavitation, in a broad sense, refers to ultrasonically induced bubble activity occurring in a biological material that contains pre-existing gaseous inclusions. Cavitation-related mechanisms include radiation force, microstreaming, shock waves, free radicals, microjets and strain. It is more challenging to deduce the causes of mechanical effects in tissues that do not contain gas bodies. These ultrasonic biophysics mechanisms will be discussed in the context of diagnostic ultrasound exposure risk concerns.

Keywords

Ultrasonic biophysics; Ultrasonic bioeffects; Ultrasonic dosimetry; Thermal mechanism; Non-thermal mechanism

1. Ultrasonic biophysics

Ultrasonic biophysics is the study of mechanisms responsible for how ultrasound and biological materials interact. As shown in Fig. 1, the study of how ultrasound affects biological materials can be viewed as bioeffect studies that can lead to therapeutic applications and risk assessments for diagnostic ultrasound applications. On the other hand, the study of how tissue affects the ultrasound wave can be viewed as the basis for diagnostic ultrasound imaging. Thus, an

†A contribution for the HPA/ICNIRP International Workshop, "Effects of Ultrasound and Infrasound Relevant to Human Health," October 24–26, 2005, Chilton, Oxfordshire, UK.

*Tel.: +1 217 333 2407; fax: +1 217 244 0105. *E-mail address:* wdo@uiuc.edu.

understanding of the interaction of ultrasound with tissue provides the scientific basis for image production, therapeutic applications and risk assessment.

Ultrasonic dosimetry (O'Brien, 1978,1986,1992b) is concerned with the quantitative determination of the interaction of ultrasonic energy with biological materials, that is, defining the quantitative relationship between some physical agent and the biological effect it produces. To understand more fully ultrasonic dosimetry and ultrasonic interaction mechanisms, it is appropriate to first introduce basic ultrasonic quantities, and then develop common nomenclature. Then, general dosimetric concepts will be presented because a large body of literature and history exists to quantitate the interaction of various propagated energies and biological materials. Ultrasonic dosimetry and its current status will be presented. To conclude, interaction mechanisms, both thermal and non-thermal, are discussed.

2. Basic ultrasonic quantities

Sound is the rapid motion of molecules. These molecular vibrations transport energy from a transmitter, a sound source like our voice, to a receiver like our ear. Sound travels in waves that transport energy from one location to another. When the molecules get closer together, this is called compression, and when they separate, this is called rarefaction. This mechanical motion, the rapid back and forth motion, is the basis for calling sound a mechanical wave or a mechanically propagated wave.

2.1. Acoustic spectrum

We have many perceptions of the nature of sound. The idea of pitch refers to our perception of frequency, that is, the number of times a second that air vibrates in producing sound that we hear. Voices are classified according to pitch in which the lowest frequency is a bass voice and the highest frequency is a soprano voice. This description of frequency, however, is limited to the frequency range, or spectrum, over which human beings can hear sounds. There are sound frequencies below and above what human beings can hear. The acoustic spectrum is shown in Fig. 2a. The lowest frequency classification in the acoustic spectrum is infrasound that has a frequency range less than about 20 Hz. Audible sound is what human beings hear and has an approximate frequency range between 20 Hz and 20 kHz. The ultrasound frequency range starts at a frequency of about 20 kHz. Examples of devices that emit frequencies at the lower frequency end of the ultrasonic spectrum are a dog whistle and industrial ultrasonic cleaners. The frequency designations of the infrasound-audio boundary and the audio-ultrasound boundary are a bit arbitrary because the frequency range over which human beings hear sounds is different between people and additionally changes as a function of age.

Most medical ultrasound equipment operates in the ultrasonic frequency range between 1 and 15 MHz (Fig. 2b). Therapeutic (physical therapy, high-frequency focused ultrasound and ablation) applications operate around 1 MHz. For most diagnostic applications in abdominal, obstetrical and gynecological ultrasound, and in echocardiography, the frequency range is generally between 2.5 and 7.5 MHz. For superficial body parts, such as the thyroid and the eye, and peripheral vascular applications where ultrasound does not have to penetrate very deeply into the body, higher ultrasonic frequencies in the range of 7.5–15 MHz can be used because ultrasonic attenuation increases with increasing frequency.

2.2. Acoustic wave types

The classification of sound waves is based on the type of motion that is induced in the medium by the propagating sound wave. For purposes of ultrasonic physics, the lowest level of organization within a fluid (gas and liquid) is called a particle (Pierce, 1981;Kinsler et al., 1982). The particle is represented in Fig. 3 as dots and can be thought of as a volume of material.

Each of these dots consists of millions of molecules and yet each has dimensions of a fraction of an ultrasonic wavelength.

When an ultrasonic wave is propagated within material, the type of wave is classified in terms of the direction the ultrasonic energy is traveling relative to the direction the particle is moving. A longitudinal wave occurs when the particles move back and forth (that is, left to right and back—horizontally in Fig. 3a) relative to the direction of the wave energy that is also moving horizontally. Propagated longitudinal waves travel through all kinds of materials: gases, liquids and solids.

In the case of shear waves, the particles move at right angles to the direction of the wave propagation as shown in Fig. 3b. In this figure, the particles are moving vertically up and down while the wave energy is moving horizontally. Shear waves exist only in solid materials, not in fluids. Shear waves do not exist in soft tissues because soft tissues are approximated as a liquid. Shear waves do, however, travel in harder biological materials such as bone.

The physical and thus ultrasonic properties of tissue are influenced by and composed of water, ions, macromolecules and cells and are a consequence of the chemical structures of fibrous and non-fibrous components. Tissues are divided into various kinds, including epithelial, muscular, connective, nervous, blood, etc. Each of these tissue types has different physical properties. Common to all tissues is a large amount of water. Selected physical properties of pure water at 37 °C (98.6 °F) are listed in Table 1 (Nyborg, 1975). The physical properties of tissue depend strongly upon water because water makes up almost three-quarters of the entire mass of the human body. The water concentration varies from tissue to tissue with vitreous humor quite high at around 99%, liver at 70%, skin at 60%, cartilage at 30% and adipose as low as 10%.

2.3. Acoustic waveforms

The nomenclature of acoustic waveforms is used to define and quantify the ultrasonic wave that interacts with biological materials.

Ultrasound travels in waves that emanate from a source. The high crests and low troughs represent specific amplitude values of the wave and correspond to peak compressional and peak rarefactional values. The distance from one crest to the next, or from one trough to the next, has a particular distance associated with it and is called the wavelength and denoted by λ in Fig. 4a. The time that it takes for one cycle to occur is called the period (Fig. 4b). The period (T) is the reciprocal of frequency ($f = 1/T$).

The horizontal axis can illustrate either distance (Fig. 4a) or time (Fig. 4b). This is an important concept in diagnostic ultrasonic instrumentation. Distance information can be converted to time values, and time converted to distance information. Ultrasonic instruments are constantly performing these conversions in order to display sonographic images. The space (or distance) over which one cycle travels is called the wavelength and the time which one cycle occupies is called the period, that is, wavelength is “distance/cycle” and period is “time/cycle.” Speed is the constant that relates wavelength (λ) to period ($T = 1/f$): $c = \lambda f$. For medical applications, the propagation speed, c, in tissue is typically assumed to be constant at 1540m/s.

There are two basic generation modes of ultrasound used in medical ultrasound (Fig. 5). Generation mode means the way in which the ultrasonic wave is “shaped” when it is transmitted from the ultrasonic transducer, that is, the waveform's temporal characteristics. One generation mode is to continuously excite the ultrasonic transducer with an electrical sine wave at constant amplitude. This produces a continuous ultrasonic wave at the same frequency as that of the

electrical frequency and is termed continuous wave ultrasound (CW mode or CW ultrasound), as shown in Fig. 5a.

Another generation mode is to turn on the ultrasound for a short time duration and turn it off for a much longer time duration and then to repeat this process. This generation mode is accomplished by exciting or shocking the ultrasonic transducer with very short electrical signals, waiting for some time and then repeating the electrical shocking. The ultrasonic waves that are generated are termed pulse wave ultrasound (PW mode or PW ultrasound), as shown in Fig. 5b. If the number of cycles per pulse is N, then the pulse duration (τ) is

$$\tau = NT = \frac{N}{f}. \tag{1}$$

The ratio of the pulse duration to the pulse repetition period (PRP) is called the duty factor (DF). The DF is the fractional amount of time that the pulse is activated, and given by

$$\mathrm{DF} = \frac{\tau}{\mathrm{PRP}} = \tau \mathrm{PRF}, \tag{2}$$

where PRF is the pulse repetition frequency. For example, if the pulse duration is 1 ms and the pulse repetition period is 1 ms (PRF = 1 kHz), then the duty factor is 0.001, or 0.1%.

A measured 2.5-MHz center frequency ultrasound pulse is shown in Fig. 6; note how nonlinear the waveform appears. The maximum value of the ultrasonic waveform, at a magnitude of about 10 MPa, occurs when the particles are compressed (at positive pressure). Thus, this value is called the peak compressional pressure amplitude. The minimum value of the ultrasonic waveform, at a magnitude of about −4 MPa, occurs when the particles are rarefied (at negative pressure). Thus, this value is called the peak rarefactional pressure amplitude, and has the value of 4 MPa (no minus sign).

2.4. Acoustic propagation speed, impedance and attenuation

An understanding of the issues related to propagation speed, impedance and attenuation in biological materials are directly applicable to the mathematical descriptions of biophysics mechanisms.

The propagation properties generally used to describe quantitatively the propagation of ultrasound in materials are speed, impedance and attenuation. The propagation of ultrasound is assumed to be an adiabatic process, that is, a process in which heat conduction does not occur. Therefore, the speed at which ultrasonic energy propagates in a fluid is (Pierce, 1981;Kinsler et al., 1982;Hall, 1987)

$$c = \sqrt{\frac{B_{\mathrm{AD}}}{\rho}}, \tag{3}$$

where the elastic modulus for an isotropic fluid is B_{AD}, the adiabatic bulk modulus and the medium's density is ρ. As such, ultrasonic waves propagated in fluids are longitudinal waves. For a gas, $B_{\mathrm{AD}} = \gamma P_0$, where γ is the ratio of specific heats and P_0 is the ambient (equilibrium) pressure, and thus

$$c = \sqrt{\frac{\gamma P_0}{\rho}}. \tag{4}$$

For a liquid, the elastic modulus is $B_{\mathrm{AD}} = \gamma B_{\mathrm{T}}$, where B_{T} is the isothermal bulk modulus and, therefore,

$$c = \sqrt{\frac{\gamma B_{\mathrm{T}}}{\rho}}. \tag{5}$$

In an isotropic solid, both longitudinal and shear waves are supported wherein their respective propagation speeds are

$$c_L = \sqrt{\frac{Y(1-\sigma)}{\rho(1+\sigma)(1-2\sigma)}} \tag{6a}$$

and

$$c_S = \sqrt{\frac{Y}{2\rho(1+\sigma)}}, \tag{6b}$$

where Y is the Young's modulus and σ is the Poisson's ratio. Because σ is less than 0.5, c_L is greater than c_S.

The specific acoustic impedance of the wave is defined as the ratio of the acoustic pressure to particle velocity. For plane waves, the specific acoustic impedance is

$$Z_S = \pm \rho c, \tag{7}$$

where + is for the positive-going wave and − is for the negative-going wave. For other than plane waves, Z_S generally different, that is, Z_S depends upon both the medium and the wave type (plane, cylindrical, spherical, etc). The ρ*c* product is encountered frequently in analytic acoustics and is called the *characteristic acoustic impedance* (*Z*) of the medium or simply the acoustic impedance. Only for a plane wave are these two impedances numerically the same. The unit of the acoustic impedance is the rayl (kg/m^2 s), after Lord Rayleigh. Table 2 summarizes the numerical ranges of ρ, *c* and *Z* for the various media.

The classical engineering trade-off of diagnostic ultrasound instrumentation is that between resolution and the depth of the image (or penetration). Both are directly affected by the ultrasonic frequency and attenuation. As frequency is increased, resolution improves and penetration decreases. Resolution improves because the ultrasonic wavelength in tissue decreases (becomes a smaller number). Wavelength is inversely related to frequency; increase one and the other decreases.

As frequency increases, the ultrasonic attenuation also increases. Penetration is directly affected by tissue attenuation because it is approximately linearly related to frequency. At an ultrasonic frequency of 1 MHz, the attenuation coefficient is approximately 0.7 dB/cm whereas at 2 MHz, it is 1.4 dB/cm. Thus, attenuation coefficient is related to frequency; increase one and the other increases. It can be expressed mathematically by the expression 0.7 dB/cm MHz, a value that approximately represents soft tissue.

2.5. Acoustic waveform quantities in a medium

A necessary concept to understand axial (or range) resolution is the distance one cycle (and hence one pulse) occupies in a medium. The distance one cycle occupies in a medium is the wavelength, λ = c/f , where *c* is the propagation speed in the medium. For a repeated pulse waveform (Fig. 5b), the distance one pulse occupies in a medium is called the spatial pulse length (SPL), that is, the number of wavelengths per pulse where

$$\mathrm{SPL} = N\lambda = \frac{\tau}{T}\lambda = \tau f \lambda. \tag{8}$$

Axial resolution is the ability to resolve discrete structures along the beam axis. Quantitatively, it is represented as the minimum distance between two structures at different ranges at which both can just be discretely identified as two separate structures. The best axial resolution is represented by the expression

$$\text{best axial resolution} = \frac{\mathrm{SPL}}{2} = \frac{N\lambda}{2}. \tag{9}$$

The transducer design affects the minimum number of cycles. More highly damped transducers (also referred to as low *Q* transducers) produce very few cycles of ultrasound when excited by the pulser voltage. As the frequency increases, and other quantities remain constant, axial resolution improves. The term “best axial resolution” has been employed because, in practice, the receiving and processing electronics affect axial resolution, as does the quality of the video monitor. The electronics and monitor are often lumped into the term “system *Q*.” Low-valued system *Q*'s provide better axial resolution than do high-valued ones. As a “rule of thumb,” there are *Q*/2 cycles of pressure contained in the pulse, that is, $N = Q/2$, which yields

$$\text{best axial resolution} = \frac{N\lambda}{2} = \frac{N}{2}\frac{c}{f} = \frac{Q}{4}\frac{c}{f} = \frac{c}{4\Delta f}, \tag{10}$$

where the quality factor *Q* is defined as the ratio of the center frequency, *f*, to the system bandwidth, Δ*f*. For a propagation speed of 1540 m/s,

$$\text{best axial resolution (in mm)} = \frac{0.77}{\Delta f}, \tag{11}$$

where Δ*f* is in MHz.

However, ultrasound images are speckle images and therefore a more representative expression for axial resolution is

$$\text{FWHM}_A\text{(in mm)} = \frac{1.37}{\Delta f}, \tag{12}$$

where FWHM_A is the axial full-width half-maximum length of the pulse in millimeters and Δ*f* is in MHz. This expression is also only a function of the system bandwidth but yields a numerical value for axial resolution about 1.8 times greater than the best axial resolution. Thus, the axial resolution improves (its numerical value decreases) when the bandwidth increases.

Lateral resolution is the ability to resolve discrete structures perpendicular, or lateral, to the beam axis. Quantitatively, it is represented as the minimum distance between two side-by-side structures at the same range at which both can just be discretely identified as two separate structures. The best lateral resolution is equal to the minimum beam width; the best lateral resolution term is employed here for the same reasons as that of the term best axial resolution. For a focused ultrasonic field, the beam width (BW) at the focus is

$$\text{BW} = 1.4\lambda\frac{\text{ROC}}{D} = 1.4\lambda f^{\#}, \tag{13}$$

where ROC is radius of curvature (in measurement practice ROC is the distance between the source and the center of the focal region, the focal length) and *D* is the diameter for a circular source or linear end-to-end lengths for a rectilinear source. In imaging terminology, the term “*f*-number” or “$f^{\#}$” is often used to quantitative focusing where the lower the *f*-number value, the better is the focusing. In terms of the full-width half-maximum length, the beam width at the focus is

$$\text{FWHM}_L = \frac{\lambda L}{D}, \tag{14}$$

where FWHM_L is the lateral full-width half-maximum length and *L* is the focal length (basically the same as ROC.

3. First- and second-order quantities

There are many buzzwords to describe a general class of events such as the terms *first*- and *second-order quantity*. *Quantity* represents what is measured and the value of a quantity is generally expressed as the product of a number and a *unit* (Table 3).

First-order quantities are known as amplitude quantities and second-order quantities as energy-based quantities (Table 4). The basic ideas of first- and second-order quantities are (1) both first- and second-order quantities deal with the transport of energy, (2) all first-order quantities are directly proportional to each other, (3) all second-order quantities are directly proportional to each other, and (4) the product of any two first-order quantities is directly proportional to any second-order quantity.

Acoustic wave propagation, and the development of its wave and other equations (Morse and Ingard, 1968;Nyborg, 1978;Pierce, 1981;Kinsler et al., 1982;Hall, 1987;Ensminger, 1988;O'Brien, 1992a;Blackstock, 2000), can be approached from the *Equation of State* which relates the change in density to the change in pressure, the *Continuity Equation* which relates particle motion to the change in density by invoking conservation of mass and the *Momentum Equation* (becomes *Euler's Equation* for a lossless medium at rest) which relates the change in pressure to particle motion through Newton's Second Law of Dynamics by invoking conservation of momentum. These equations and their various forms are: Equation of State

$$p = c_0^2 \delta\rho\left\{1 + \frac{B}{2!A}\frac{\delta\rho}{\rho_0} + \frac{C}{3!A}\left(\frac{\delta\rho}{\rho_0}\right)^2 + \cdots\right\}, \tag{15a}$$

$$p = c_0^2 \delta\rho\left\{1 + \frac{B}{2!A}s + \frac{C}{3!A}s^2 + \cdots\right\}. \tag{15b}$$

Continuity Equation

$$\frac{\mathrm{D}\rho}{\mathrm{D}t} + \rho\nabla \cdot \vec{u} = 0, \tag{16a}$$

$$\frac{\partial \rho}{\partial t} + \nabla \cdot (\rho\vec{u}) = 0. \tag{16b}$$

Momentum Equation

$$\rho\frac{\mathrm{D}\vec{u}}{\mathrm{D}t} + \nabla P = 0, \tag{17a}$$

$$\rho_0\frac{\partial \vec{u}}{\partial t} + \nabla p = 0 \text{ (linear Euler's Equation)}. \tag{17b}$$

The total or material derivative is

$$\frac{\mathrm{D}q}{\mathrm{D}t} = \frac{\partial q}{\partial t} + (\vec{u}.\nabla)q, \tag{18}$$

where the first term on the right-hand side is the time rate of change of q (any first-order acoustic variable) the fluid particle would experience if it were at rest ($\vec{u} = 0$), and the second term is the additional rate of change caused by the particle's movement. Also, p is the acoustic pressure (instantaneous pressure $P = P_0 + p$), δ_ρ is the excess density (instantaneous density $\rho = \rho_0 + \delta_\rho$), B/A is the coefficient of the first nonlinear parameter (Beyer, 1997), s is the condensation, the fractional change in density (δ_ρ/ρ_0) and $\vec{u}$ is the particle velocity of a fluid element.

Pressure P, velocity $\vec{u}$, density ρ can be expressed as

$$P = P_0 + p_1 + p_2 + \ldots, \tag{19a}$$

$$\vec{u} = \vec{u}_1 + \vec{u}_2 + \ldots, \tag{19b}$$

$$\rho = \rho_0 + \rho_1 + \rho_2 + \ldots, \tag{19c}$$

where the subscripts indicate the order. For example, P_0 is the zero-order contribution to pressure, p_1 is the first-order contribution that varies sinusoidally for a harmonic (CW) wave at frequency ω, and $p2$ is the second-order contribution that has both a temporal-dependent component at frequency 2ω and a temporal-independent component. Because the fluid is assumed to be at rest, the zero-order contribution to $\vec{u}$ is zero.

3.1. First-order quantities

The Equation of State, the Continuity Equation and the Euler's Equation for first-order contributions become, respectively,

$$p_1 = Bs_1 + \eta_B \frac{\partial s_1}{\partial t}, \tag{20}$$

$$\frac{\partial s_1}{\partial t} = -\nabla \cdot \vec{u}_1, \tag{21}$$

$$\rho_0 \frac{\partial \vec{u}_1}{\partial t} = -\nabla p_1. \tag{22}$$

In water and tissue, $n_B(\partial s_1/\partial t)$[unk]$Bs_1$. Thus, the Equation of State becomes $p_1 = Bs_1$. Eliminating the order 1 subscripts and noting that $\vec{u} = \mathrm{d}\xi / \mathrm{d}t$, where ξ is the particle displacement, by combining these equations for a one-dimensional wave propagating in the x direction yields the one-dimensional lossless wave equation

$$\frac{\partial^2 \xi}{\partial t^2} = c^2 \frac{\partial^2 \xi}{\partial x^2}. \tag{23}$$

The one-dimensional lossless wave equation can be described by the particle displacement ξ (x, t), or can likewise be described by the particle velocity u(x, t), the particle acceleration a (x, t), or the acoustic pressure p(x, t). In terms of the particle displacement, the one-dimensional lossless wave equation traveling in the positive x direction is represented as

$$\xi(x, t) = \xi_0 \cos(\omega t - kx), \tag{24}$$

where ξ_0 is the particle displacement amplitude, ω is the angular frequency, t is time and k is the wave number (also called the propagation constant).

For plane waves, particle velocity, particle acceleration and acoustic (ultrasonic) pressure are determined, respectively, from

$$u(x, t) = \frac{\partial \xi(x, t)}{\partial t}, \tag{25}$$

$$a(x, t) = \frac{\partial u(x, t)}{\partial t}, \tag{26}$$

$$p(x, t) = -\rho c^2 \frac{\partial \xi(x, t)}{\partial x}, \tag{27}$$

where Eq. (27) is determined by combining the Equation of State and the Continuity Equation to yield $p = \rho_0 c^2 s$, where $s = -\partial\xi/\partial x$ for a plane wave. All first-order plane wave ultrasonic amplitude quantities are directly proportional to each other. These quantities are

$$\xi_0 = \frac{U_0}{\omega} = \frac{A_0}{\omega^2} = \frac{p_0}{\omega \rho_0 c_0}, \tag{28}$$

where U_0, A_0 and p_0 are the particle velocity amplitude, particle acceleration amplitude and acoustic (ultrasonic) pressure amplitude, respectively.

For the lossy one-dimensional wave equation, the medium's attenuation coefficient is part of the solution wherein

$$\xi(x, t) = \xi_0 e^{-Ax} \cos(\omega t - kx), \tag{29}$$

where A is attenuation coefficient.

3.2. Second-order quantities

When an ultrasound wave propagates in tissue, a mechanical strain is induced, where strain refers to the relative change in dimensions or shape of the body that is subjected to stress. From the second-order contribution to the Momentum Equation (Eq. (17)), the gradient of P, ∇P, a force quantity, is

$$\vec{F} = \rho \frac{\mathrm{D}\vec{u}}{\mathrm{D}t}, \tag{30}$$

where $\vec{F}$ is a temporal and spatial varying force per volume (in $\mathrm{N/m^3}$), the volume being a fluid element.

Also, ultrasonic wave propagation transports and dissipates energy, and second-order quantities are proportional to energy. Quantitatively, energy is represented in terms of energy density (a scalar) and intensity (a vector). For a plane wave propagating in the x direction, the instantaneous kinetic and potential energies are, respectively,

$$E_{\mathrm{KE}}(x, t) = \frac{\rho u^2}{2}, \tag{31}$$

$$E_{\mathrm{PE}}(x, t) = \frac{p^2}{2\rho c^2}, \tag{32}$$

where u and p are the respective instantaneous values of particle velocity and acoustic pressure.

To evaluate the temporal-average energy density, the one-dimensional, harmonically varying particle velocity is assumed to be

$$u(x, t) = U_{\mathrm{op}} \cos(\omega t - kx) + U_{\mathrm{on}} \cos(\omega t + kx), \tag{33}$$

where U_{op} and U_{on} are the particle velocity amplitudes for the positive and negative directed components, respectively, and the one-dimensional, harmonically varying ultrasonic pressure is

$$p(x, t) = p_{\mathrm{op}} \cos(\omega t - kx) + p_{\mathrm{on}} \cos(\omega t + kx), \tag{34}$$

where $p_{\mathrm{op}} = \rho c U_{\mathrm{op}}$ and $p_{\mathrm{on}} = -\rho c U_{\mathrm{on}}$. Therefore, the average energy density is

$$\langle E \rangle = \frac{1}{T}\int_0^T E(x, t)\,\mathrm{d}t = \frac{\rho}{2}\left(U_{\mathrm{op}}^2 + U_{\mathrm{on}}^2\right). \tag{35}$$

Intensity is an extremely useful ultrasonic quantity that represents a measure of ultrasonic power flowing (temporal-average rate of flow of energy) at normal incidence to a specified unit area. The intensity concept is generally applied in connection with a traveling plane wave. Further, it is a vector quantity but, because the development herein is confined to a fluid and to the one-dimensional wave equation, vector notation is not used; the direction is known. The instantaneous intensity is defined as the dot product of the ultrasonic pressure and particle velocity but because these two quantities are in phase, the dot product is pu. Its temporal-average representation is given by

$$I = \frac{1}{T}\int_0^T pu\,\mathrm{d}t = \frac{\rho c}{2}\left(U_{\mathrm{op}}^2 - U_{\mathrm{on}}^2\right). \tag{36}$$

It should be noted that for a standing wave where $U_{op}^2 = U_{on}^2$, the temporal-average intensity (a vector) is zero whereas the temporal-average energy density (a scalar) is not.

For a progressive ultrasonic plane wave propagating in only the positive *x* direction, $U_{on}^2 = 0$, Eqs. (35) and (36) become, letting $U_{op}^2 = U_0^2$,

$$\langle E \rangle = \frac{\rho}{2} U_0^2 = \frac{1}{2\rho c^2} p_0^2 \tag{37}$$

and

$$I = \frac{\rho c}{2} U_0^2 = \frac{1}{2\rho c} p_0^2 = \frac{p_0 U_0}{2}, \tag{38}$$

where $\langle E \rangle$ is the temporal-average energy density (in J/m^3 or N/m^2) and I is the temporal-average intensity (in W/m^2 or, more conventionally in ultrasonic biophysics, W/cm^2). Combining these results yields

$$\langle E \rangle = \frac{I}{c}, \tag{39}$$

which is a useful expression in terms of measuring ultrasonic intensity and ultrasonic power with radiation force techniques, but only valid for plane waves.

The temporal-average energy density is equivalent to the radiation force (in *N*) for a perfect absorber in that

$$F_{rad} = \frac{IA}{c}, \tag{40}$$

where *A* is the area of the absorber. The product term *IA* is acoustic power *W*, thus,

$$F_{rad} = \frac{W}{c}. \tag{41}$$

For a perfect reflecting surface, the radiation force is twice that of an absorbing target.

If the medium is lossy, and the loss is assumed to be purely absorptive with an absorption coefficient α, then for a one-dimensional wave propagating in the positive *x* direction, the particle velocity (from Eqs. (25) and (29)) and temporal-average intensity can be described by

$$u(x, t) = U_0 e^{-\alpha x} \sin(\omega t - kx), \tag{42}$$

$$I = I_0 e^{-2\alpha x}, \tag{43}$$

where I_0 is the intensity at $x = 0$. From these two expressions, and the temporal-average value of $\vec{F}$ (Eq. (30)), the temporal-average radiation force on the medium is

$$F_{rad} = \frac{2\alpha I}{c}. \tag{44}$$

4. Dosimetry

Dosimetry is the determination of a dose, or similar type of physical quantity, that characterizes the physical agent as to its potential or actual interaction with the biological material of interest. Ultrasonic dosimetry's objective is to relate magnitudes of specific quantities, such as intensity, acoustic pressure, particle displacement, etc., or perhaps some quantity yet to be developed, to the likelihood of occurrence of a biological alteration. To accomplish this, it is necessary (1) to quantify the output quantity or quantities of the source, (2) to determine the effect of the

material on the propagating energy, viz., reflections, refraction, scattering, absorption, etc., and (3) to relate quantitatively the first two items at the site of interest.

Typically, dose connotes something that is given or imparted in a quantitative manner. The history of other radiation forms has documented that defining dose, or dose-like concepts, is difficult, especially when the objective is to include all possible physical and biological variables. More commonly, however, special quantities are developed for the biological action under consideration. In ionizing radiation, for example, dose generally refers to the quantity *absorbed dose* that has been defined as the energy imparted to matter by ionizing radiation per unit mass of irradiated material at the site of interest (ICRU, 1971;CGPM, 1975,1976). But other dose quantities have been defined for specific purposes such as genetically significant dose, cumulative dose, dose equivalent, threshold dose, etc. (BEIR, 1972,2005). In photobiology, dose sometimes refers to the quantity *dose of ultraviolet radiation* which has been defined as the energy per unit surface area applied to an object (Rupert, 1974). There has been much discussion regarding microwave dosimetry. Terms such as specific absorption rate, absorbed power density and specific absorption density and energy dose-rate have been used as a basic quantity to describe absorbed electromagnetic energy (Anderson, 1992;Bernhardt, 1992;Grandolfo, 1992;Leonowich, 1992;Sliney, 1992).

By comparison, the field of ultrasonic dosimetry has not developed nearly to the extent of ionizing radiation dosimetry. The most widely used quantity in ultrasonic bioeffect and biophysical studies is intensity in the unit of W/cm^2. The principal reason for the use of intensity is, perhaps, convenience because it is understood how it is measured (IEEE, 1990;Lewin and Schafer, 1992). However, intensity represents many of the same problems as does the ionizing radiation quantity “exposure” in that it is not a measure of dose. Yet the majority of bioeffect and biophysical reports use intensity as the measured physical quantity of the ultrasonic field. This extensive literature documents the actions of ultrasound but, in most cases, lacks the necessary characterization of the field at the site of interest. An ideal situation would be to know the instantaneous particle velocity, the instantaneous acoustic pressure and the phase between these two field parameters at the site or sites of interest (O'Brien et al., 1972;O'Brien, 1978,1986,1992b).

There have been early ultrasonic dosimetric quantities that are noteworthy of comment in that they represent, in concept, the basic approach to dosimetry. The *cataract-producing unit*, CPU, was a quantity defined as the duration of exposure necessary to produce a grossly observable cataract and expressed in units of seconds (Purnell et al., 1964). The dosimetric concept *damage ability index* with the unit second is a quantity intended to describe the effect of ultrasound on spinal cord hemorrhage (Taylor and Pond, 1972). It has been suggested (Johnston and Dunn, 1976) that a universal dosimetric response to ultrasonic exposure may exist for different tissues but the response has only been demonstrated, in a limited manner, in mammalian brain tissue. The response was in terms of *energy absorbed per unit volume* for histologically observable lesions at superthreshold levels as a function of the *delivered intensity*. It was shown that at two different ultrasonic frequencies, 3 and 4 MHz, identical constant volume curves resulted even though there were two different threshold levels (Dunn and Fry, 1971). Later, a damage integral was defined to predict the occurrence and dimensions of thermally induced ophthalmic lesions (Lizzi et al., 1984).

In another category of ultrasonic dosimetric studies, in utero ultrasonic intensity in both the gravid and non-gravid human uterus has been estimated (summarized in Stewart and Stratmeyer, 1982;NCRP, 1983). In these early studies, a model of the tissue layers between the skin surface and fetal sac yielded a total attenuation in the range of 2–20 dB at frequencies between 2 and 5 MHz. The distances between the abdominal surface and the uterine cavity in

early pregnancy ranged between 2 and 11 cm. In later work (Carson et al., 1989), similar distances were estimated to be 2.6 cm.

In human-based studies wherein direct in utero ultrasonic pressure measurements were made (Daft et al., 1990;Siddiqi et al., 1991), the average attenuation was reported to be 6.2±3.5 dB under full bladder conditions and 7.3±4.9 dB under empty bladder conditions. Applying the fixed-attenuation tissue model (attenuation dependent upon frequency and independent of distance), and normalizing to the center frequency of 2.4 MHz, the attenuation coefficient was estimated to be 2.56±1.47 dB/MHz for the full bladder condition whereas, with the overlying tissue model (attenuation dependent upon frequency and non-fluid distance), the attenuation coefficients were estimated to be 0.89±0.71 dB/cm MHz and 0.45±0.32 dB/cm MHz, respectively, for full and empty bladder conditions. The mean values for the fixed-attenuation tissue model's attenuation coefficient were about a factor of 3 greater than the values proposed to model the attenuation coefficient by Carson et al. (1989). FDA's Center for Devices and Radiological Health uses a value of 0.3 dB/cm MHz as a derating factor (a tissue attenuation coefficient) for manufacturers in their 510(k) process to estimate ultrasonic intensity quantities in tissue (FDA, 1985;Harris, 1992). The measured mean values for the overlying tissue model's attenuation coefficient were a factor of 2–3 greater than the values used by FDA suggesting that FDA's values error on the side of safety.

In general, it is necessary to determine a firm database from which various dosimetric modeling approaches can be explored. In one approach (Carson et al., 1989), a worst-case approach was employed to overestimate safety whereas, in another approach (Siddiqi et al., 1991), the mean values of the results and their distributions were reported so that the scientific community could make the appropriate safety judgments. But for ultrasonic dosimetry, neither an approach to monitor energy absorbed per unit mass nor to monitor the biological danger have yet been developed. The only adopted approach is that developed in the *Standard for Real-Time Display of Thermal and Mechanical Indices on Diagnostic Ultrasound Equipment*, commonly known as the Output Display Standard (ODS) and its revisions (ODS, 1992,1998,2004), and discussed below under thermal (Section 6) and non-thermal (Section 7) mechanisms.

5. A brief history

The development of the mechanisms responsible for ultrasound-induced biological effects is closely linked to the unique history of the development of diagnostic ultrasound applications in human medicine and the basis for the development of standards (O'Brien, 1998). A brief overview of the historical development of ultrasonic biophysics is thus provided. In many cases, the same pioneers whom development ultrasound applications also elucidated the ultrasound biophysical mechanisms.

More than three decades after the 1880 discovery of the piezoelectric effect by the brothers Paul-Jacques and Pierre Curie (Curie and Curie, 1880), a discovery which revolutionized the production and reception of high-frequency sound, the French scientist Paul Langevin developed one of the first uses of ultrasound for underwater echo ranging of submerged objects with a quartz crystal at an approximate frequency of 150 kHz (Hunt, 1982). Langevin was, perhaps, the first to observe that ultrasonic energy could have a detrimental effect upon biological material wherein he reported (Langevin, 1917) “fish placed in the beam in the neighborhood of the source operation in a small tank were killed immediately, and certain observers experienced a painful sensation on plunging the hand in this region.” Langevin also reported observing incipient cavitation in water when the source was active.

Another decade passed before a more detailed, experimental study was conducted (Wood and Loomis, 1927) to investigate Langevin's (1917) observation. Although the ultrasonic levels were not specified, their experimental studies showed that ultrasonic energy had a range of

effects from rupture of Spirogyra and Paramecium to death of small fishes and frogs by a 1–2-min exposure, the latter also observed by Langevin with a Poulsen arc oscillator. Considerable work followed and in the earliest review paper on this subject, Harvey (1930) reported on the physical, chemical, and biological effects of ultrasound in which alterations were produced in macromolecules, microorganisms, cells, isolated cells, bacteria, tissues, and organs with a view towards the identification of the interaction mechanisms. The ultrasonic exposure conditions of these early works were neither well characterized nor reported, but the exposure levels were undoubtedly high.

Ultrasound-induced tissue heating was applied extensively as a therapeutic agent in the 1930s and 1940s. However, while it was clear that ultrasound could effectively heat tissue, and excess enthusiasm resulted in numerous clinical applications being proposed and tried, the inferior clinical experience caused this modality to fall into disfavor (see discussion of 1949 Erlangen resolution (Kremkau, 1979)). Thus, as Hill (1973) observed of this time, “it is perhaps unfortunate that the generation of ultrasound proved to be so relatively simple and cheap that a considerable practice was built up.”

Also, during the 1930s and 1940s, with an understanding that ultrasound at sufficient levels could have a dramatic effect on tissues, and produce large temperature increases, the potential for ultrasonic surgery was proposed. This ability to non-invasively burn focal tissue volumes deep in the body using ultrasound was first proposed in 1942 (Lynn et al., 1942,1944) as a neurosurgery technique. Ultrasound surgery and its biophysical mechanism (heating) were further developed in the late 1940s and early 1950s (Fry et al., 1955). Also proposed in 1948 and applied in 1952 was the application of ultrasound surgery to destroy the vestibular function to treat the symptoms of Menie`re's disease (Sjoberg et al., 1963).

While ultrasound exposimetry was inferior in these early times to that possible today, these early bioeffect studies clearly demonstrated that ultrasound, at sufficient levels, could easily destroy biological material. From the earliest considerations that ultrasound might be a feasible energy source for producing images of the human body, it was known that high ultrasonic energy levels had the potential to be hazardous. This information must be kept in mind because many of the early pioneers who were developing ultrasound imaging devices were also cognizant that ultrasound had the potential for disrupting biological materials. Additionally, they were aware from the history of ionizing radiation to be concerned with the potential for hazardous effects. Thus, it must be presumed that there has been a continuing concern of the risk from ultrasound prior to and during the entire period of diagnostic instrumentation development.

During the 1950s and 1960s, the ability to quantify ultrasonic fields improved but only to a limited extent; there were still no nationally based ultrasound measurement standards or procedures. All of the improvements dealt with absolute procedures to quantify second-order quantities, and consisted of ultrasonic intensity via thermocouple probe (Fry and Fry, 1954a,b;Fry and Dunn, 1957;Dunn and Breyer, 1962) and electrodynamic method (Filipczynski, 1967), and ultrasonic power via radiation pressure and calorimetry (Wells et al., 1963) and radiation pressure balance (Newell, 1963;Kossoff, 1965).

It should be noted that as early as 1951 (French et al., 1951), individuals working on the development of diagnostic ultrasound equipment had an awareness of a potential risk to patients. Also in the early 1950s the same investigators active in image system developments were also investigating the nature of ultrasound-induced tissue damage (Fry et al., 1950, 1951,1970;Hueter et al., 1956;Baum, 1956), thus demonstrating a concern for the safety of this diagnostic modality.

This period saw only a few advances in our understanding of how ultrasound interacted with biological materials. Perhaps the first major symposium on “Ultrasound in Biology and Medicine” was held at the University of Illinois in 1952 to examine phenomena of how ultrasonic energy interacted with and acted upon biological materials. Of the eight papers presented, six were published and dealt with the effects of high-intensity ultrasound (Fry, 1953;Wall et al., 1953;Wild and Reid, 1953) or the thermal mechanism of ultrasound (Fry and Fry, 1953;Herrick, 1953;Lehmann, 1953). Two additional symposia were held (June, 1955, 1962) to address similar issues (Kelly, 1957,1965). This literature laid the basic foundation for the biophysical mechanisms by which ultrasound is known to affect biological materials, viz., thermal and cavitation.

There were scattered reports about ultrasound having an effect on biological systems during this period, but these reports in general did not deal with the types of exposure that would be expected from diagnostic ultrasound equipment, nor did they provide any kind of a consistent message. Two summaries identify a number of these early reports (Reid and Sikov, 1972;Stewart and Stratmeyer, 1982). However, during the 1950s and 1960s, as diagnostic ultrasound equipment started to be used in clinical medicine, there continued to be concerns about its safety, which could not be dispelled because of the paucity of well-conducted and comprehensive experimental studies.

One interesting observation made in the late 1960s that would wait more than two decades before it would become an active area of basic and clinical research was the identification of the production of cavitation at the tip of catheters when various liquids were injected through the catheter. The cavitation was a primary source of echoes in an echocardiograph image, and the first application of an injected contrast agent was identified (Kremkau, 1969;Kremkau et al., 1970).

The 15-year period between early 1970s and mid-1980s witnessed the greatest expansion with diagnostic ultrasound imaging capabilities, starting with bistable, static and ending with gray-scale, real-time capabilities. During this period, the ability to quantify ultrasonic fields improved considerably. Perhaps the first intercomparison (between two universities) to assess the absolute measurement of ultrasonic intensity was conducted (Breazeale and Dunn, 1974); the comparison was conducted with the elastic sphere radiometer (Dunn et al., 1977). A major breakthrough of earlier work (Brain, 1924;Fukada, 1968) occurred with Kawai's discovery in 1969 (Kawai, 1969) of the strong piezoelectric effect in polyvinylidenefluoride (PVDF) to measure the temporal characteristics of diagnostic ultrasound fields. Two types of PVDF hydrophones were developed, viz., needle (Lewin, 1981) and membrane (DeReggi et al., 1981;Bacon, 1982;Harris, 1982;Preston et al., 1983). The US National Bureau of Standards (now the National Institute of Standards and Technology, NIST) developed an ultrasound power transfer standard (Fick et al., 1984), and the UK National Physical Laboratory developed both a two-transducer reciprocity technique and an optical technique (Smith, 1986).

This 15-year period had its controversies relative to whether diagnostic ultrasound was safe. Two of the controversies are briefly reviewed to illustrate the level of concern the ultrasound community felt because these reports dealt with the potential of diagnostic ultrasound affecting chromosomes. In 1970 it was reported that ultrasound from a low-output commercial fetal pulse detector-induced aberrations in human lymphocyte chromosomes (Macintosh and Davey, 1970,1972). Numerous laboratories throughout the world attempted to replicate the findings without success. The matter was brought to closure when, in 1975, the same lead author of the original report was invited to another laboratory in an attempt to duplicate the experiment; they were unable to reproduce the original findings (Macintosh et al., 1975). In the late 1970s, a report appeared (Liebeskind et al., 1979) which suggested that exposure from a diagnostic ultrasound system showed an increase in human lymphocyte sister chromatid

exchange (SCE) frequency (an indication of chromosome damage). Like with the previous chromosomes aberration situation, numerous laboratories throughout the world attempted to replicate the findings. In 1984, the American Institute of Ultrasound in Medicine's Bioeffects Committee carefully and thoroughly reviewed a total of 14 ultrasound-SCE studies and concluded that these studies do not suggest a hazard from exposure to diagnostic ultrasound (Goss, 1984).

In the early to mid-1970s, there was great uncertainty with respect to the safety of ultrasound as discussed above and what authority and role the US Food and Drug Administration (FDA) would take in terms of regulating diagnostic ultrasound. Regulatory control of diagnostic ultrasound in the United States can be traced to passage of the 1976 Medical Device Amendments to the Food, Drug and Cosmetic Act, but for the several years prior to its passage, the FDA coordinated a classification scheme for all medical devices. There was apprehension among the public, patients, physicians, sonographers, basic scientists, manufacturers, and the government. One of the fundamental difficulties was the lack of an accurate and precise procedure to quantify diagnostic ultrasound equipment outputs. Because of these difficulties, the output levels from diagnostic ultrasound equipment were not well characterized, and human exposure levels could not be compared to results from laboratory experimental studies. In response to this uncertainty, and the lack of a suitable measurement scheme, the American Institute of Ultrasound in Medicine (AIUM), a medical and scientific professional society, and the National Electrical Manufacturers Association (NEMA), a trade organization that represented many of the ultrasound manufacturers, joined efforts in 1976 to develop a voluntary standard that would assure that sufficient information on the characteristics of diagnostic ultrasound equipment was supplied to allow medical personnel to make informed judgments regarding the application of this equipment to patients. The *Safety Standard for Diagnostic Ultrasound Equipment* (AIUM/NEMA, 1983) was developed over a 5-year period and set forth precise definitions, output measurement procedures and labeling requirements related to those characteristics of ultrasound equipment that were believed at that time to pertain to patient exposure and safety. The voluntary standard's labeling requirements called for manufacturers to make available (publicize) to the ultrasound community the maximum values of the following ultrasonic quantities: ultrasonic power; spatial peak, temporal average intensity (I_{SPTA}); and spatial peak, pulse average intensity (I_{SPPA}). The labeling requirements were based on the philosophy that there was a *potential risk* from diagnostic ultrasound exposure and included those quantities whose magnitudes were known or believed to be related to actual damage or to risk of damage to biological tissues; they were the quantities most often reported in the basic science literature to relate the strength of ultrasound to the production of biological effects in laboratory experimental studies. The voluntary standard did not specify upper limits.

In the early1980s, the pioneering observations by Apfel (1981a,1982,1986), Flynn (1982) and Flynn and Church (1988) from their mathematical models to describe the dynamic behavior of small bubbles (or microbubbles) in liquids suggested the strong possibility for transient cavitation (now termed inertial cavitation) to occur from microsecond pulses of ultrasound. This opened up the scientific debate that cavitation in tissue might occur from diagnostic ultrasound exposures.

Also in the early 1980s, the assessment of diagnostic ultrasound risk was addressed by two major activities. One of the activities was sponsored by the US National Institutes of Health consensus development conference processes (NIH, 1984) by convening an expert panel of physicians, basic scientists, epidemiologists, nurses, educators, and sonographers to provide answers to specific questions related to safety and efficacy of diagnostic ultrasound in obstetric practice. The document indicated that the increasing use of ultrasound during pregnancy is safe and effective for 28 medical conditions. This was, perhaps, the first time that the issue of diagnostic ultrasound efficacy was critically reviewed. Also, this process recommended against

routine scanning of the embryo and fetus. Further, it was suggested that while diagnostic ultrasound does not appear to be associated with any known hazards, investigators should continue to evaluate risks.

The other activity was conducted under the auspices of the National Council on Radiation Protection and Measurements (NCRP, 1983). The document rigorously covered the basic physics of ultrasound with an emphasis on medical ultrasound fields and on the quantification of various ultrasonic field quantities to which humans were exposed during the course of an ultrasound examination. Also included were mechanisms by which ultrasound interacts with biological material and effects caused by ultrasound on biological materials such as plants, animals, and in vitro systems. Finally, this document set forth a number of recommendations that fell into the categories of research needs, industrial practices, education, and exposure criteria. It is interesting that a number of the recommendations were consistent with those put forth by the Workshop on the Interaction of Ultrasound and Biological Tissues (Reid and Sikov, 1972) a decade earlier.

When the FDA initiated the regulation of diagnostic ultrasound equipment in the mid-1980s (FDA, 1985), it set *application-specific* intensity limits in their 1985 “510(k) premarket notification” which manufactures could not exceed (Table 5). This notification is used by the FDA to determine if the new devices are substantially equivalent, in safety and effectiveness, to diagnostic ultrasound devices on the market prior to May 28, 1976, the date when the Medical Device Amendments were enacted. The exposure quantities required by FDA were, in part, similar to those in the *Safety Standard for Diagnostic Ultrasound Equipment* voluntary standard's labeling requirements (AIUM/NEMA, 1983). However, the limits were not based on safety considerations but rather on the maximum output limits of known diagnostic ultrasound equipment at the time when the Medical Devices Amendments were enacted, in May, 1976; hence the term *pre-amendments levels* (O'Brien et al., 2002).

To emphasize the date-base regulation approach as opposed to the safety- and efficacy-base regulation approach of the FDA, the American Institute of Ultrasound in Medicine notified the FDA in mid-1986 (AIUM, 1986) that there existed prior to May 28, 1976 at least two diagnostic ultrasound devices (pre-enactment ultrasound devices) with intensity levels greater than those listed in Table 5. In early 1987, the FDA updated their diagnostic ultrasound guidance to higher intensity levels (FDA, 1987) to those listed in Table 6. The date-based regulation approach has been criticized by technical, scientific, and medical professionals, as well as by the diagnostic ultrasound industry (Merritt, 1989) because of the implication that these arbitrary limits are safety based, and because they could limit future clinical benefits by preventing the development of more advanced diagnostic ultrasound systems, and hence greater clinical benefit, that may require higher output levels. Further, it must be recognized that limited diagnostic ultrasound capabilities may, in fact, be responsible for greater risk to the patient due to either an inadequate diagnosis, or to the use of an additional diagnostic procedure with a defined risk.

Within the past decade or so, there have been substantial improvements, through national and international efforts, in our understanding to identify the biological interactions diagnostic ultrasound exposures may have with soft tissues, including both thermal (NCRP, 1992;WFUMB, 1992;AIUM, 1993) and acoustic cavitation-like (AIUM, 1993,2000;WFUMB, 1996) phenomena. These reports have provided, in part, the basis for the development of a new approach to regulate diagnostic ultrasound equipment (see Sections 6.2 and 7.1).

It had been long thought that diagnostic ultrasound exposures could not produce biological damage. However, in the early 1990s, based on initial observations in the late 1980s from lithotropsy experiments, diagnostic ultrasound-type pulses at diagnostic pressure levels have

produced significant damage (lung hemorrhage) in mice, rats, rabbits, and monkeys, the first observation being in mice (Child et al., 1990). There are open questions yet about whether this effect occurs in humans.

Ultrasonic biological effect studies and biophysical research have shown that ultrasound can produce changes in living systems. The *AIUM/NEMA Ultrasound Safety Standard for Diagnostic Ultrasound Equipment* (AIUM/NEMA, 1983) and *AIUM Acoustic Output Measurement and Labeling Standard for Diagnostic Ultrasound Equipment* (AIUM/NEMA, 1992) labeling requirements were based on the philosophy that there is a possible risk from diagnostic ultrasound exposure. The specific labeling requirements of these and other (Harris, 1992) safety standards were selected to include those quantities whose magnitudes are known or believed to be related to actual damage or to risk of damage to biological tissues as a result of ultrasonic irradiation.

The basis for this rationale lies in an understanding of the mechanisms by which it is known that ultrasound can affect living systems. Such knowledge comes from fundamental laboratory studies (O'Brien, 1984,1991;O'Brien and Withrow, 1985). These mechanisms are classified and discussed in terms of whether heat is or is not believed to be the principal cause for the biological effect. The applicable ultrasonic exposure quantities are identified during the course of this discussion. Both thermal and non-thermal mechanisms are considered.

6. Thermal mechanism

Whenever ultrasonic energy is propagated into an attenuating material such as tissue, the amplitude of the wave decreases with distance. This attenuation is due to either *absorption or scattering*. Absorption is a mechanism that represents that portion of the wave energy that is converted into heat, and scattering can be thought of as that portion which changes direction. Because the medium can absorb energy to produce heat, a temperature increase may occur as long as the rate at which heat is produced is greater than the rate at which the heat is removed (O'Brien, 1978;NCRP, 1983,1992,2002). The thermal mechanism is relatively well understood because increase in temperature produced by ultrasound can be calculated using mathematical modeling techniques (Robinson and Lele, 1972;Nyborg, 1975,1981;Lerner et al., 1973;Cavicchi and O'Brien, 1984,1985;Nyborg and Steele, 1983;Nyborg and O'Brien, 1989;Curley, 1993;Lubbers et al., 2003) and has been estimated for a variety of exposure conditions (NCRP, 1983,1992).

In tissue, at the site where the ultrasonic temporal-average intensity is I_{TA}, the rate of heat generation per unit volume is given by the expression (Nyborg, 1981;Cavicchi and O'Brien, 1984)

$$\dot{Q} = 2\alpha I_{TA} = \frac{\alpha p p^*}{\rho c}, \tag{45}$$

where

$$I_{TA} = \frac{p p^*}{2\rho c}, \tag{46}$$

where α is the ultrasonic amplitude absorption coefficient which increases with increasing frequency, p and p^* are the instantaneous ultrasonic pressure and its complex conjugate, respectively, ρ is density and c is sound speed. The product of p and p^* is equal to the ultrasonic pressure amplitude squared, p_0^2, at the specific location in the medium where $\dot{Q}$ is determined and can be thought of as a temporal-average quantity.

The temporal-average intensity is not necessarily at the location where it is maximized, that is, at the spatial peak location. If it were, however, then I_{TA} (Eq. (46)) would be the spatial peak, temporal peak intensity I_{SPTA}, which would maximize $\dot{Q}$ for that tissue site. AIUM's Statement on Mammalian In vivo Ultrasonic Biological Effects (Table 7), sometimes referred to as the *100 mW/cm^2 Statement*, is a generalization about the state-of-affairs with respect to an intensity–time limit (in terms of I_{SPTA}) below which there have been no independently confirmed significant biological effects in mammalian tissues (AIUM, 1988).

For a given I_{TA}, the maximum temperature increase $\Delta T_{max,}$ under the assumption that no heat is lost by conduction, convection, or any other heat removal processes, is approximately described by (Fry and Fry, 1953)

$$\Delta T_{max} = \frac{\dot{Q}\Delta t}{C_v}, \tag{47}$$

where Δt is the time duration of exposure and C_v is the medium's heat capacity per unit volume. This formula is valid only for short exposure times; for longer exposure times, heat removal processes become significant. Nonetheless, as a "ballpark estimate," using the intensities from the *AIUM Statement* in Table 7 of I_{SPTA} = 0.1 and 1 W/cm^2 at an ultrasonic frequency of 5 MHz, from Eq. (45), $\dot{Q} = 0.05$ and 0.5 J/cm^3 s ($\alpha \approx 0.25$/cm at 5 MHz). Because the thermal properties of biological tissue can be approximated by water (C_v = 4.18 J/cm^3 °C), the maximum rates of change of temperature are

$$\frac{\Delta T_{max}}{\Delta t} = 0.012 \text{ and } 0.12\ ^\circ\text{C/s}, \tag{48}$$

which means that for a 1 s exposure, ΔT_{max} would be about 0.012 and 0.12 °C. If the exposure duration were longer than 1 s, the temperature would continue to increase but at a progressively slower rate, until the rate of heat generation was about the same as the rate of heat removal.

To estimate the temperature increase from a single pulse for clinical, diagnostic pulse-echo instrumentation, the local, single pulse intensity of Eq. (45) is considered to be the spatial peak value averaged over the duration of the pulse, that is, the spatial peak, pulse average intensity, I_{SPPA}. For typical instrumentation, a maximum value of I_{SPPA} may be as high as 500 W/cm^2. Thus, the maximum time rate of change of temperature is

$$\frac{\Delta T_{max}}{\Delta t} = 60\ ^\circ\text{C/s}, \tag{49}$$

but, with a diagnostic pulse duration, Δt, of approximately 2 μs, the maximum temperature rise, $\Delta T_{max} \approx 120$ μ°C. However, in the case of high-intensity focused ultrasound (HIFU) for which the pulse duration may be as long as 3 s (ter Haar, 2004), Eq. (49) clearly demonstrates that the temperature increase could exceed levels sufficient to ablate tissue.

In living tissue, heat transfer occurs partly by perfusion (i.e., blood flow) and partly by conduction (also called diffusion). A widely used thermal model for tissue is the bioheat transfer equation (Pennes, 1948), a formulation that includes a source/sink term that accounts for heat transfer from blood perfusion, that is,

$$\frac{\partial T}{\partial t} = \kappa \nabla^2 T - \frac{\Delta T}{\tau} + \frac{\dot{Q}}{C_v}, \tag{50}$$

where $\delta T/\delta t$ is the rate of temperature increase at a point, κ is the thermal diffusivity, T is the temperature, ΔT is the temperature increase above ambient, and τ is the perfusion time constant.

Even though the bioheat transfer equation has shortcomings (Weinbaum et al., 1984), it is easy to implement analytically and is perhaps the most widely used thermal model of living tissue. Analyses based on the bioheat transfer equation (NCRP, 1983;Curley, 1993) were used to develop some of the ODS's thermal indices (ODS, 2004).

There have been several studies to calculate the temperature increase in mammalian tissue from ultrasonic exposure and some of them have shown to compare favorably with experimental results (Pond, 1968,1970;Robinson and Lele, 1972;Lerner et al., 1973;NCRP, 1983;Nyborg and Steele, 1983;Cavicchi and O'Brien, 1985;AIUM, 1988,1993,2000;Smith et al., 1995). These studies demonstrate that selected aspects of the theory are reasonably well understood. But there are still many unanswered concerns in terms of being able to assess in vivo temperature increase.

6.1. Thermal dose concept

Healthy cellular activity depends upon chemical reactions occurring at the proper location at the proper rate. The rates of chemical reactions and thus of enzymatic activity are temperature dependent. The overall effect of temperature on enzymatic activity is described by the relationship known as the 10° temperature coefficient, or Q_{10} Rule (Hille, 2001). Many enzymatic reactions have a Q_{10} near 3 which means that for each 10 °C increase in temperature, enzymatic activity increases by a factor of 3; a more physical description of rate-dependent temperature effects is the Arrhenius activation energy concept (Henle, 1983;Sapareto and Dewey, 1984;Dewey, 1994;Dewhirst et al., 2003). An immediate consequence of a temperature increase is an increase in biochemical reaction rates. However, when the temperature becomes sufficiently high (i.e., approximately ≥45°C), enzymes denature. Subsequently, enzymatic activity decreases and ultimately ceases, which can have a significant impact on cell structure and function.

If damage occurs during exposure of tissue(s) to elevated temperature, the extent of damage will be dependent upon the duration of the exposure as well as on the temperature increase achieved. Detrimental effects in vitro are generally noted at temperatures of 39–43 °C, if maintained for a sufficient time period; at higher temperatures (>44 °C) coagulation of proteins can occur. These effects have been documented in experimental studies of heat-induced cell death in cultures of normal and cancerous cell lines. The lethal (100% destruction) dose (LD_{100}) for HeLa cells exposed to different temperatures for differing durations has ranged from 41 °C for 96-h duration to 46 °C for 30-min duration (Selawry et al., 1957;Hornback, 1984). These findings are comparable to the time-temperature relationship to destroy 50% (LD_{50}) of sarcoma-180 tumor cells in mice (Crile, 1961;Hornback, 1984); from 42 °C for 2-h duration to 46 °C for 7.5-min duration.

These observations suggest a logarithmic relationship between time and temperature for death due to a temperature increase. Dickson and Calderwood (1980) have indicated a similar relationship for time vs. temperature for thermal-induced death of tumors and normal animal and human tissues. Important points addressed in this study are: (1) at 40 °C long-duration exposures (5–100 h) are required for thermal-induced cell death, and (2) at temperatures appreciably below 40 °C there are no irreversible adverse effects detected.

An empirical formula, based on a large number of studies involving the thermotolerance of cells and tumors, relates the time, t (in min), required to produce an isoeffect (e.g., a given amount of cell killing) to the time (t_{43}) which would be required had the exposure occurred at a reference temperature of 43 °C, that is,

$$t_{43} = tR^{(43-T)}, \quad (51)$$

where R = 0:5 for T>43 °C and R = 0.25 for T≤43 °C (Henle, 1983;Sapareto and Dewey, 1984;Dewey, 1994;Dewhirst et al., 2003). Theoretical considerations based on reaction kinetics (thermodynamic Arrhenius analyses) led to the prediction that the temperature dependence of the rate of protein denaturation is determined primarily by the activation energy. The quantity R is an expression of the relative increase in reaction rate for a 1 °C increase in temperature. The rationale for there being two "R" values is based upon the empirical determinations of R for a number of biological systems and endpoints (Dewey et al., 1977;Sapareto and Dewey, 1984, 1994; Dewhirst et al., 2003). In these systems, R-values ranged from 0.4 to 0.8, with 0.5 being the most common value, for temperatures above 43 °C. The few studies performed at temperatures ≤43 °C indicate that the R-value is approximately one-half of the value obtained at the higher temperatures.

By using Eq. (51), the empirical relationship derived by Sapareto and Dewey (1984), an equivalent t_{43} can be ascribed to any combination of temperature and exposure duration. It also follows that any given biological effect due to hyperthermia can be characterized by that t_{43} value of the causative exposure. The lowest t_{43} value giving rise to some effect would be considered the threshold.

Miller and Ziskin (1989) estimated that the t_{43} was greater than 1 min for each teratologic observation in their study (the lowest t_{43} for any effect was 1.9 min for the production of exencephaly in the mouse (Webster and Edwards, 1984)). Rearranging Eq. (51), and assuming that R = 0:25 (for temperatures ≤43 °C), yields

$$t = t_{43} 4^{(43-T)}. \tag{52}$$

Miller and Ziskin (1989) used t_{43} = 1 min for fetal tissues, that is,

$$t = 4^{(43-T)} \tag{53}$$

and the March 26, 1997 *AIUM Conclusions Regarding Heat* statement (AIUM, 1997) used Eq. (53) (t_{43} = 1 min) to indicate that there have been no significant, adverse biological effects observed due to temperature increases less than or equal to the line definded by this equation (see Fig. 7); the applicable exposure duration ranged between 1 and 250 min.

For non-fetal tissues a range of t_{43} values has been reported. Results for breast (Lyng et al., 1991) and other tissues (Dewey, 1994) are summarized in Table 8. It should be noted that some of the data were garnered using animal models, whose core temperatures are higher than 37 °C, implying that the temperature increase necessary to achieve a particular thermal dose would be lower than would be the case with humans (Miller and Dewey, 2003;Herman and Harris, 2003). Adjustments in the t_{43} as applicable to humans might have to be made.

More generally,

$$t = t_{43} R^{(T-43)}, \tag{54}$$

where t is the time (in min) corresponding to the threshold for a specific bioeffect which results from exposure to a temperature T (in °C). Also, R = 0.5 for T>43 °C and R = 0.25 for T≤43 °C. This equation explicitly states the relationship between temperature and exposure duration on the boundary line.

Fig. 7 shows the temperature–time curves for 4 values of t_{43} (see Eq. (54)). The lower curve (t_{43} = 1 min) represents that estimated for fetal tissues for t>1 min (Miller and Ziskin, 1989;AIUM, 1997). The other three curves, based on Table 8 t_{43} values (10, 100 and 240 min), represent non-fetal tissues that are less sensitive to tissue damage from temperature. Note that the temperature values for an exposure duration of 1 min are 43.0, 44.7, 46.3 and 47.0 °C for

t_{43} values of 1, 10, 100 and 240 min, respectively. Based on the values in Table 8, the t_{43} = 1 min plot represents a conservative, tissue non-specific boundary for assessing thermal safety for non-fetal exposures.

For very short exposure times, the hyperthermia literature shows only limited (Borrelli et al., 1990) t_{43} thermal dose data points for exposure durations of less than 1 min. Two aspects of single-burst in vivo threshold lesion studies in brain (Fry et al., 1970;Dunn and Fry, 1971;Lerner et al., 1973) and liver (Chan and Frizzell, 1977;Frizzell et al., 1977;Frizzell, 1988) are germane to the thermal dose issue for exposures less than a few seconds. The threshold lesion curve for cat brain is described by the expression $It^{0.5}$ = 350 $Ws^{0.5}/cm^2$ over for exposure durations between 0.3 ms and 300 s. The threshold lesion curve for cat and rabbit liver is described by the expression $It^{0.5}$ = 460 $Ws^{0.5}/cm^2$ over for exposure durations between 3 ms and 35 s. I is the spatial peak intensity (in W/cm^2) and t is exposure duration (in sec). Thus the first aspect is that liver has a higher threshold than brain, consistent with the t_{43} thermal dose trend for brain and liver in Table 8. The second aspect is that for the brain threshold studies, an estimate was made of lesion temperature increase ΔT, yielding, at 6 MHz, $\Delta T/I$ estimates (interpolated from Fig. 4 in Lerner et al., 1973) of 0.086, 0.13 and 0.16 $°Ccm^2/W$ for pulse durations of 1, 10 and 100 s respectively. Combining these $\Delta T/I$ estimates with $It^{0.5}$ = 350 $Ws^{0.5}/cm^2$, and assuming a cat core temperature of 39 °C (NCRP, 1992), yields three temperature–time data points (open triangles on Fig. 8; also see Table 9).

In addition, there have been a number of documents that have reported threshold-based data for single-burst exposure durations as low as 100 ms (Table 9). These data are graphically shown in Fig. 8.

These data (Table 9) suggest that for non-fetal soft tissue, and for scanning conditions consistent with conventional B-mode ultrasound exams for which the exposure durations at the same in situ location would be less than a few seconds, the allowable maximum temperature increase could be relaxed relative to longer exposures.

6.2. Output display standard: thermal indices

A diagnostic ultrasound educational activity was initiated with a workshop in June, 1988. This workshop set out certain principles which resulted in the initiation of a 3-year process involving numerous clinicians, scientists, engineers and government regulators from many organizations; this group finalized and approved, in 1992, the *Standard for Real-Time Display of Thermal and Mechanical Indices on Diagnostic Ultrasound Equipment*, commonly referred to as the ODS (ODS, 1992). The purpose of this voluntary standard was to provide the capability for users of diagnostic ultrasound equipment to operate their systems at levels much higher than previously had been possible in order to have the potential for greater diagnostic capabilities; the standard did not specify any upper limits. In doing so, the possibility existed for the potential to do harm to the patient. Therefore, two biophysical indices were provided so that the equipment operator has real-time information available to make appropriate clinical decisions, viz., benefit vs. risk, and to implement the ALARA (As Low As Reasonable Achievable) principle (NCRP, 1990), that is, the ODS provides for a real-time output display which gives the user information about the potential for temperature increase (the Thermal Index (TI)) and mechanical damage (the Mechanical Index; see Section 7.1)

In the early 1990s, FDA implemented the ODS (ODS, 1992;FDA, 1993,1994,1997). While the ODS (ODS, 1992) did not specify upper limits, FDA's implementation (FDA, 1997) of the ODS stipulated regulatory upper limits of 720 mW/cm^2 for the derated (0.3 dB/cm MHz) spatial peak, temporal average intensity, $I_{SPTA.3}$, and either 1.9 for the Mechanical Index, MI or 190 mW/cm^2 for the derated (0.3 dB/cm MHz) spatial peak, pulse average intensity, $I_{SPPA.3}$. There is, however, an exception for ophthalmic application for which $I_{SPTA.3} \leq 50$ mW/cm^2 and

MI≤0.23 (FDA, 1997). In addition, FDA (1997) requires the manufacturer to justify TIs greater than 6. The ODS has been revised (ODS, 1998,2004), but FDA's regulatory upper limits have not changed.

The TI provides information about tissue temperature increase. This development addresses the thermal mechanism and closely related to the thermal mechanism is the TI. The basic TI definition is (ODS, 2004)

$$\mathrm{TI} = \frac{W_0}{W_{\mathrm{DEG}}}, \tag{55}$$

where W_0 is the source power of the diagnostic ultrasound system and W_{DEG} is the source power required to increase the tissue temperature 1 °C under very specific and conservative conditions. Three different Thermal Indices were developed to address three different tissue models and two different scan modes, that is, the soft-tissue Thermal Index (TIS), the bone Thermal Index (TIB), and the cranial-bone Thermal Index (TIC). The unscanned-mode is typically used clinically for spectral Doppler and M-Mode where the ultrasound beam remains stationary for a period of time. Also, the unscanned-mode soft-tissue TI, as well as TIB, are the only TI quantities that attempt to estimate temperature increase at locations other than at or near the source surface. The others estimate temperature increase at or near the source surface.

The following evaluation addresses the accuracy of the unscanned-mode TIS for circular (O'Brien and Ellis, 1999) and rectangular (O'Brien et al., 2004a) sources.

For the circular sources (O'Brien and Ellis, 1999), 3 source diameters (1, 2 and 4 cm) and 8 transmit *f-numbers* (ROC/source diameter = 0.7, 1.0, 1.3, 1.6, 2.0, 3.0, 4.0 and 5.0) were evaluated at 8 frequencies (1, 2, 3, 4, 5, 7, 9 and 12 MHz), yielding 192 cases. For the rectangular sources (O'Brien et al., 2004a), 33 one-dimensional focused rectangular aperture cases were investigated (Fig. 9) for which the aperture's *x*-length direction is the axis that is focused (*y*-length direction not focused) to an appropriate ROC to yield 3 *f*-numbers (ROC/*x*-length = 1, 2, and 4). Six frequencies (1, 3, 5, 7, 9 and 12 MHz) were evaluated (99/frequency), yielding 594 cases.

For all 786 cases, the medium was assumed to be homogeneous in terms of both acoustic and thermal properties). The attenuation coefficient (also referred to as a derating factor) and absorption coefficient were both 0.3 dB/cm MHz, density was 1000 kg/m^3, propagation speed was 1540 m/s, tissue perfusion length was 1 cm and tissue thermal conductivity was 6 mW/cm °C. These were the values used in the ODS (ODS, 1992,1998,2004) and the values used herein for the evaluation of the unscanned-mode TIS. They were also the values used to compute the maximum steady-state temperature increase (ΔT_{max}) and its axial location. Also, all results reported herein are based on the derated spatial-peak, temporal-average intensity $I_{\mathrm{SPTA.3}}$ of 720 mW/cm^2,FDA's (1997) regulatory limit.

Figs. 10 and 11 directly compare the 192 circular source ΔT_{max}-TIS pairs as a function of frequency and *f*/number, respectively. TIS generally underestimates (is less than) ΔT_{max} for *f-numbers* ≤2, conditions for which ΔT_{max}≤0.30 °C and TIS≤0.40. This suggests that for transmit *f-numbers* ≤2, TIS would not need to be displayed according to the ODS display requirements. With the exception of the longer-focus, larger-diameter, higher-frequency sources, TIS generally tracks ΔT_{max} for *f-numbers*≥3. These exceptions suggest a breakdown of the ODS procedures for calculating TIS.

Figs. 12 and 13 directly compare the 594 rectangular source ΔT_{max}-TIS pairs as a function of frequency and *f*/number, respectively. TIS overestimates (is greater than) ΔT_{max} for all but one of the cases.

The ODS process does not specify the location of ΔT_{max}. Figs. 14 and 15 show the relationship between ΔT_{max} and its location (axial distance) for the circular and rectangular sources, respectively, as a function of *f*-number (the same 3 *f*-numbers are shown for direct comparison). And, Figs. 16 and 17 show the relationship between ROC and its axial distance locations of ΔT_{max} for the circular and rectangular sources, respectively, as a function of *f*-number. For all 786 cases, the axial distance locations of ΔT_{max} are less than the ROC, the geometric focus location. As frequency increases for the lower *f*-number cases, the axial distance locations of ΔT_{max} move closer to the geometric focus. However, for the higher *f*-number cases in each frequency set for $f \geq 3$ MHz, the axial distance locations of ΔT_{max} jumps to near the transducer surface. This behavior, also reported by Thomenius (1990), becomes more prevalent at higher frequencies and larger source diameters. Thus, the ΔT_{max} location is not necessary near the skin surface.

In scanned modes, however, the focal energy is distributed over a large area and hence will tend to have lower spatial intensities than unscanned modes. With the recent introduction of real-time three-dimensional scanners, the focal energy will be distributed over two dimensions that should result in further reduction in relevant focal intensities. However, there will be an added concern of near-field heating. Near-field heating could be exacerbated by transducer self-heating (Duck et al., 1989). At this point it is believed that the development of a new index to cover these cases is not indicated in view of the regulatory mechanisms that are already in place for transducer surface temperatures.

The ODS process does not take into account the temporal dependency of the temperature increase. An evaluation of the temporal dependency of temperature increase was conducted for the circular sources of three source diameters (1, 2 and 4 cm) at two frequencies (2 and 7 MHz) for five *f-numbers* (*f*/1, *f*/2, *f*/3, *f*/4 and *f*/5); Fig. 18 shows $t_{80\%}$, the time when the temperature increase reaches 80% of its steady-state value *at that axial distance*, for two source diameters (1 and 4 cm). Each $t_{80\%}$ profile follows the same general pattern as a function of axial distance. For each of the 7-MHz cases, the axial distances of the minimum $t_{80\%}$ values are, in general, near the respective focal regions. However, for the 2-MHz cases, the axial distances of the minimum $t_{80\%}$ values tend not to be near the respective focal regions but rather closer to the transducer. Also, the minimum $t_{80\%}$ values increase as a function of increasing *f-number*, and decrease as a function of increasing frequency. The global minimum $t_{80\%}$ values are 97.2 and 59.7 s for the fifteen 2-MHz and fifteen 7-MHz cases, respectively, both of which are for the 1-cm-diameter, *f*/1 cases.

6.3. Output display standard: possibly better thermal indices

The TIs in use today were developed more than 14 years ago (ODS, 1992). While the ODS has been revised twice (ODS, 1998,2004), the TI equations have not changed. Figs. 10-13 indicate that there could be improvements. There has been one effort to improve the unscanned-mode TIS. The database used was the same as that used to develop for the 594 rectangular source cases (O'Brien et al., 2004a), and yielded two new TIS expressions:

$$\mathrm{TIS}_{\mathrm{new}}(1) = \frac{W_0^{0.85} f_c^{0.58}}{169 \cdot A_{\mathrm{aprt}}^{0.33}}, \qquad 56$$

$$\mathrm{TIS}_{\mathrm{new}}(2) = \frac{W_0^{0.73} f_c^{0.62}}{130}, \qquad 57$$

where W_0 is the source power in millwatts (in mW), f_c is the center frequency in megahertz (in MHz) and A_{aprt} is the active aperture area (in cm^2) (see Fig. 19). In both models, only the source power and frequency need to be measured; they can adequately be measured (AIUM/NEMA, 1998). The only difference between $TIS_{new(1)}$ and $TIS_{new(2)}$ is the degree of agreement with ΔT_{max} that might be required.

7. Non-thermal mechanisms

Both first- and second-order quantities have been implicated in non-thermally produced biological effects (NCRP, 2002). The non-thermal mechanism that has received the most attention is acoustically generated cavitation, principally from ultrasound contrast agent microbubbles. Excellent reviews of cavitation have been published (Flynn, 1964,1975a,b, 1982;Nyborg, 1965,1975;Coakley and Nyborg, 1978;Apfel, 1981b;NCRP, 1983,1992, 2002;Leighton, 1994;ter Haar and Duck, 2000;AIUM, 2000;Suslick, 2001;Hoff, 2001). Effects have been also attributed to radiation force. There is also a class of ultrasound-induced biological effects that have not yet been determined to be due to either thermal or a specific non-thermal mechanism.

7.1. Output display standard: mechanical index

The Mechanical Index, MI, is defined as

$$\mathrm{MI} = \frac{p_{r.3}}{\sqrt{f}}, \tag{58}$$

where $p_{r.3}$ is the derated peak rarefactional pressure in MPa (megapascals) and f is the ultrasonic frequency in MHz. The derating factor (attenuation coefficient of soft tissue) is assumed to be 0.3 dB cm MHz. The development of the Mechanical Index was based on theoretical and in vitro experimentation by investigators (Holland and Apfel, 1989;Apfel and Holland, 1991) who discovered a simple relationship between acoustic pressure and the onset of cavitation under an assumption that the optimum bubble size is present. The theory assumed isothermal growth, adiabatic collapse, an incompressible host fluid and neglected gas diffusion into the bubble, and the experiments were conducted in an aqueous medium, not tissue. These observations were the basis for the adoption of the MI (ODS, 1992).

7.2. Radiation force

Within recent times, a number of ultrasound diagnostic techniques have emerged that use the static or dynamic acoustic radiation force to locally move and/or vibrate tissue including acoustic radiation force impulse imaging (Nightingale et al., 1995,2001), vibro-acoustography (Fatemi and Greenleaf, 1998,1999), supersonic shear imaging (Bercoff et al., 2004). Generally, these techniques utilize the ultrasound-induced temporal-average force on the medium (Section 3.2) to elicit a biophysical effect (tissue motion). The magnitude of the effect is proportional to the local temporal-average intensity. Whether there are other biophysical effects (risk-related temporary or permenant tissue responses) have not been extensively studied.

However, the ultrasound-induced temporal-average force has been implicated as a mechanism associated with tactile response (Gavrilov et al., 1977a,b;Gavrilov, 1984;Magee and Davies, 1993;Dalecki et al., 1995), auditory response (Foster and Wiederhold, 1978;Tsirulnikov et al., 1988), increased fetal activity (Arulkumaran et al., 1991,1996;Fatemi et al., 2001), bone repair (Dyson and Brookes, 1983;Wang et al., 1994,2001), cardiac changes in frogs (Dalecki et al., 1993,1997a), movement of detached retinas (Lizzi et al., 1978) and macroscopic streaming to differentiate between cystic and solid tumors (Stavros and Dennis, 1993;Nightingale et al., 1995). Other than those responses related to macrostreaming (Nyborg, 1953,1965), there is a limited association, possibly only speculative, between the response and radiation force.

7.3. Cavitation without injected microbubbles

When an ultrasound wave propagates in tissue, a mechanical strain is induced, where strain refers to the relative change in dimensions or shape of the body that is subjected to stress. The strain is significant near gas or vapor bubbles, hence the interest in ultrasound-induced cavitation. Cavitation, in a broad sense, refers to ultrasonically induced activity occurring in a liquid or liquid-like material that contains bubbles or pockets containing gas or vapor. These bubbles originate within materials at locations termed “nucleation sites,” the exact nature and source of which are not well understood in a complex medium such as tissue. Under ultrasonic stimulation, the bubble oscillates and at sufficiently high ultrasonic pressure levels, the bubble can collapse. Collapse cavitation is termed “inertial collapse” because the bubble motion is dominated by the inertia of the liquid. There are some excellent treatments of bubble dynamics and inertial cavitation (Gilmore, 1952;Flynn, 1975a,b,1982;Keller and Miksis, 1980;Apfel, 1981b;Flynn and Church, 1988;Matsumoto and Watanabe, 1989;Prosperetti and Lezzi, 1986;AIUM, 2000;NCRP, 2002;Church 2002,2005). Cavitation can affect a biological system by virtue of a temperature increase, a mechanical stress, and/or free radical production. Even so, this is traditionally referred to as a non-thermal mechanism.

The occurrence of cavitation, and its behavior, depends on many factors, including: the ultrasonic pressure; whether the ultrasonic field is focused or unfocused, or pulsed or continuous; to what degree there are standing waves (i.e., energy reflecting back onto itself); and the nature and state of the material and its boundaries. Experimentally, because cavitation would probably affect only a single or a few cells, it would be extremely difficult to detect an adverse biological effect, unless the cavitation events were widespread among a large volume of tissue. The latter has been shown to be the case when mammalian nervous system tissue was exposed to ultrasonic levels in excess of I_{SPTP} of 1000 W/cm^2 for a pulse duration of at least 1 ms (Dunn and Fry, 1971;Frizzell, 1988); these conditions are outside of the diagnostic equipment range.

Theoretical predictions suggested that inertial cavitation could occur in liquids by diagnostic ultrasound exposures provided that appropriate cavitation nuclei were present (Apfel, 1982, 1986;Flynn, 1982;Apfel and Holland, 1991). The minimum threshold for inertial cavitation was calculated for the diagnostically relevant frequency range (Apfel and Holland, 1991), and this theory served as the basis for the ODS's Mechanical Index (ODS, 1992). A theoretical prediction considered the possibility of spontaneous nucleation in tissue modeled as a homogeneous liquid, in the absence of preexisting nuclei, wherein a frequency-independent (1–15 MHz) rarefactional pressure threshold was on the order of 4 MPa (Church, 2002). However, soft tissue is a viscoelastic material, not a pure liquid, and recent theoretical predictions suggest that inertial cavitation thresholds are higher for soft tissue than liquids (Yang and Church, 2005). Thus, there has been no experimental evidence to suggest that inertial cavitation events occur in mammalian parenchymal tissue from exposure-like conditions employed with diagnostic ultrasound equipment, that is, endogenous cavitation nuclei are rare in most tissues.

7.4. Cavitation with injected microbubbles

The principal medical application of ultrasound contrast agents (UCAs) is to enhance the echogenicity of blood. Such ultrasound contrast agent microbubbles provide preexisting nuclei and thus the possibility for ultrasound-induced cavitation and potential for bioeffects. In the United States, Albunex® (Molecular Biosystems, Inc., San Diego, CA) was the first FDA-approved UCA in 1994. An improved version of Albunex®, Optison™ (then MBI, San Diego, CA), was FDA approved in 1997. The only other 2 FDA-approved UCAs are Definity® (Bristol-Meyers Squibb, NY, NY) in 2001 and Imagent® (IMCOR, San Diego, CA) in 2002. Other UCAs have been approved in Canada and/or Europe (Miller and Nanda, 2004), but since

2002 there have been no new UCAs approved by FDA. While there are no written documents, it appears that FDA is uncertain about UCAs' safety and appears to be waiting until more is known about the device risk of these agents.

Three ultrasound exposure modes are used with UCAs, viz., low MI, normal MI and high MI, where MI is the Mechanical Index (ODS, 2004), to create 3 imaging phenomena (Miller and Nanda, 2004). Low MI is considered around 0.1 and the UCAs undergo linear oscillations. Normal MI is considered between 0.2 and 0.7 and the UCAs undergo nonlinear oscillations. High MI is considered between 0.8 and 1.9 [FDA's regulatory limit (FDA, 1997)] and the UCAs undergo destruction. For normal MI and high MI, it is thought that the UCA signals are bubble-specific.

It is unfortunate that the MI has become the UCA exposure quantity, but the MI is an exposure quantity available to system operators. The concept is well founded, but the science is weak because the MI is a water-based measurement, not an in situ measure of ultrasonic pressure. For the same displayed MI, the in situ ultrasonic pressure varies as a function of the interposed tissue attenuation coefficient and thickness. Also, what ultrasonic pressures (thresholds) are necessary to collapse UCAs in vivo are unknown.

Using a passive cavitation detector, UCA rupture based on ultrasonic emissions from single Optison™ UCAs have been measured (Fig. 20) (Ammi et al., 2004,2006;Wang et al., 2006). Ultrasonic pulses were transmitted into weak solutions of Optison™. Signals detected with a 13-MHz center-frequency transducer revealed post-excitation ultrasonic emissions (between 1 and 5 ms after excitation) with broadband spectral content. The observed ultrasonic emissions were consistent with the US signature that would be anticipated from inertial collapse followed by “rebounds” when an UCA ruptures and thus generates daughter/free bubbles that grow and collapse. The peak rarefactional pressure threshold for detection of these emissions increased with frequency ($p<0.0001$), but the apparent threshold decrease with increasing pulse duration was not statistically different. The estimated MI thresholds at the 4 frequencies of 0.9, 2.8, 4.6 and 7.1 MHz (Fig. 20) were 0.6, 0.7, 0.7 and 0.9, respectively, well within the diagnostic ultrasound exposure levels (FDA, 1997).

Concerns about the potential bioeffects of inertial cavitation associated with the interaction of ultrasound with contrast agents in human beings have been addressed (AIUM, 2000;NCRP, 2002). These concerns were raised by studies documenting hemolysis of erythrocytes in vitro in cell suspensions that contained contrast agent and in vivo in mice injected with intravenous contrast agent that were exposed to pulsed ultrasound (Williams et al., 1991;Dalecki et al., 1997b;Miller et al., 1997;Miller and Gies, 1998a,b;Poliachik et al., 1999;Brayman and Miller, 1999). In vitro studies have reported damage to monolayers of cultured cells whose culture media contained contrast agent and were exposed to pulsed ultrasound (Brayman et al., 1999a;Ward et al., 1999;Miller and Bao, 1998;Miller and Quddus, 2000a). Hemorrhage in the vascular beds of the intestine and skin (Miller and Quddus, 2000b;Miller and Gies, 2000) and damage to cells in the heart (Skyba et al., 1998) were also demonstrated in mice and dogs, respectively, following intravenous injection of contrast agent and exposure to pulsed ultrasound. In vivo studies have reported induction of petechiae and hemolysis (Killam et al., 1998;Skyba et al., 1998;Miller and Quddus, 2000b;Wible et al., 2002;Hwang et al. 2005), damage to the intestinal wall (Miller and Gies, 1998a,b,2000;Kobayashi et al., 2002,2003), and alteration to the blood-brain barrier (Schlachetzki et al., 2002;Hynynen et al., 2003).

More medically significant have been the reports of arrhythmogenic changes that included premature ventricular contractions in healthy adult human beings during triggered second harmonic imaging of a UCA for myocardial perfusion (van Der Wouw et al., 2000); supraventricular tachycardia or non-sustained ventricular tachycardia in patients at risk for

syncope, supraventricular tachycardia, or ventricular tachycardia after intravenous administration of UCA and exposure to therapeutic transthoracic low-frequency ultrasound (Chapman et al., 2005); and cardiac arrhythmogenesis in a rat model (Zachary et al., 2002). Cavitation has been suggested as the likely mechanism for microbubble-induced premature cardiac contractions (Dalecki et al. 2005).

In addition, there are also a number of possible therapeutic benefits of UCAs. A significant problem in cancer chemotherapy is the compromised quality of life experienced by the patient due to the side effects of these drugs. Delivery of drugs directly and specifically to solid tumors is often inefficient, and as a result, the patient's healthy cells and tissues are subject to the toxic effects of the drugs. Thus, it is important to develop therapeutic strategies that deliver drugs to the appropriate cells within the patient in a way that is specific, efficient, and safe. One such method involves the use of US to enhance cell permeability. With this method, it is possible via the vasculature of the tumor, to deliver therapeutic compounds placed within UCAs directly to tumor cells when the tumor is insonated with US and the UCAs are ruptured. In addition, when exposed to US, the membrane of a cell can become transiently permeable. This effect, termed sonoporation, is enhanced when UCAs undergo cavitation near the cells. Small compounds (Brayman et al., 1999b;Guzman et al., 2001;Kayhani et al., 2001), macromolecules (Guzman et al., 2002;Miller et al., 1999), DNA (Bao et al., 1997;Greenleaf et al., 1998;Wyber et al., 1997;Amabile et al., 2001;Lawrie et al., 2000;Miller et al., 2003;Miller and Song 2003), protein (Mukherjee et al., 2000;Weimann and Wu, 2002), and other therapeutic compounds (Harrison et al., 1996;Kayhani et al., 2001;van Wamel et al., 2004) have been delivered into cells using US. This membrane alteration can be transient (McNeil, 1989), leaving the compounds trapped inside the cell after US exposure. Thus, sonoporation is a viable delivery method, ensuring site-specific drug delivery or transfection.

Even though this section deals with non-thermal mechanisms, UCAs can have an effect on bulk tissue heating (Hilgenfeldt et al., 1998,2000;Chavrier and Chapelon, 2000;Holt and Roy, 2001;Sokka et al., 2003;Umemura et al., 2005). Typically, there is at least a 2–4 times enhancement of tissue heating by cavitation, or, if the bioeffect were a lesion, the lesion volume was likewise enhanced. Also, single bubbles undergoing inertial collapse can cause plasma formation and temperature elevation (≈4300–5000 K) sufficient to induce thermal injury (Didenko et al., 1999;Suslick, 2001). Additionally, such high temperatures in an aqueous medium may result in the formation of chemically reactive free radicals (Verral and Sehgal, 1988) that can cause damage.

7.5. Ultrasound-induced lung hemorrhage

One of the most extensively studied ultrasound-induced biological effects is lung hemorrhage. However, the mechanism is not clear. While heating resulting from the absorption of ultrasound can cause tissue injury, heating has been experimentally excluded as the mechanism responsible for ultrasound-induced lung hemorrhage via thermocouple measurements (Hartman et al., 1992). A thermal mechanism has also been excluded via a pathological evaluation of laser-induced lung lesions (Zachary et al., 2006). Also, inertial caviation has been excluded as the mechanism using an overpressure procedure (O'Brien et al., 2000) and the injection of contrast agents (O'Brien et al., 2004b). Some general observations can be made, however, from the extensive number of ultrasound-induced lung damage threshold studies.

Fig. 21 shows all of occurrence threshold findings across four species using the same methodology [mouse (Zachary et al., 2001a), rat (Zachary et al., 2001a;O'Brien et al., 2001, 2003b), rabbit (O'Brien et al., 2006), and pig (O'Brien et al., 2003a)]. Pre-2000 occurrence threshold findings (Fig. 22) across three species [mouse (Child et al., 1990;Raeman et al., 1993,1996;Frizzell et al., 1994;Dalecki et al., 1997d), rat (Holland et al., 1996), pig (Baggs et al., 1996;Dalecki et al., 1997c)] have also been reported (AIUM, 2000) for which experimental

techniques and statistical approaches were different from the statistical analysis procedure (Simpson et al., 2004) used with Fig. 21 experiments. A principal difference between the two sets of studies lies in the exposure duration wherein Fig. 21 threshold findings used a 10-s ED while the pre-2000 threshold findings (Fig. 22) used typically longer EDs. The 10-s ED yielded occurrence thresholds typically higher (median: 3.0 MPa; range: 1.2–5.8 MPa) than the pre-2000 thresholds (median: 1.0 MPa; range: 0.4–2.5 MPa).

All of these occurrence threshold values (from Figs. 21 and 22) have been organized as a function of frequency (Fig. 23 relative to ultrasonic pressure and Fig. 24 relative to Mechanical Index). Virtually every ultrasound-induced lung hemorrhage threshold is less than the FDA regulatory limit (MI<1.9, FDA 1997), that is, within the diagnostic ultrasound frequency range. These thresholds are over a wide range of animal weights [mouse: 22–32 g, rat: 190–330 g, rabbit: 1.9–2.9 kg, and pig: 1–25 kg] and chest wall thicknesses [mouse: 1.9–4.9 mm, rat: 4.1–6.0 mm, rabbit: 5.0–6.6 mm, and pig: 2–22 mm].

The results of the studies using mice, rats, rabbits and pigs have shown two important facts relative to the biological mechanisms of damage: (1) there are no differences in biological mechanism of injury induced by ultrasound based on species and age; therefore, structural differences among mammalian species studied are independent of the biological mechanism that causes ultrasound-induced lung damage and (2) lesions induced by ultrasound are similar in morphology in all species and age groups studied, and the character of the lesions is independent of frequency, PRF, and beamwidth. These findings suggest that the mechanism of injury is similar in all species and age groups. It is thus plausible to speculate that the same biological mechanism causing ultrasound-induced lung hemorrhage in laboratory animals may be in play in human beings undergoing sonographic procedures with direct or incidental exposure of lung, especially patients with pulmonary disorders and “at risk” neonates. However, the extent of ultrasound-induced lung damage, and the ability of the lung to heal (Zachary et al., 2001b), lead to the conclusion that while diagnostic ultrasound can produce lung damage at clinical levels, the degree of damage does not appear to be a significant medical problem.

Acknowledgments

This work was supported by NIH Grant R37EB02641. Also acknowledged is the American Institute of Ultrasound in Medicine for the sponsorship of the 2005 AIUM Bioeffects Consensus Conference from which the author derived considerable insight for this contribution.

References

AIUM. Letter from AIUM president and AIUM standards committee chair to director, FDS's CDRH Office of Device Evaluation and Acting Director. FDA's CDRH Office of Science and Technology. June 23;1986 1986

AIUM. Bioeffects considerations for the safety of diagnostic ultrasound. J. Ultrasound Med (September) 7;1988 :S1–S38. [PubMed: 3054148]

AIUM. Bioeffects and Safety of Diagnostic Ultrasound. American Institute of Ultrasound in Medicine, AIUM Publications, American Institute of Ultrasound in Medicine; 14750 Sweitzer Lane, Suite 100, Laurel, MD 20707, USA: 1993.

AIUM. AIUM Conclusions Regarding Heat statement. AIUM Publications, American Institute of Ultrasound in Medicine; 14750 Sweitzer Lane, Suite 100, Laurel, MD 20707, USA: 1997.

AIUM. Mechanical bioeffects from diagnostic ultrasound: AIUM consensus statements. J. Ultrasound Med (February) 19;2000 :68–168.

AIUM/NEMA. Safety standard for diagnostic ultrasound equipment. AIUM/NEMA Standards Publication No. UL 1-1981. J. Ultrasound Med 1983;2:Sl–S50.

AIUM/NEMA. AIUM Acoustic Output Measurement and Labeling Standard for Diagnostic Ultrasound Equipment. American Institute of Ultrasound in Medicine; Rockville, MD: 1992.

AIUM/NEMA. Acoustic Output Measurement Standard for Diagnostic Ultrasound Equipment. American Institute of Ultrasound in Medicine; Laurel, MD: 1998. and National Electrical Manufacturers Association, Rosslyn, VA

Amabile PG, Lewis JM, Lewis TN. High-efficiency endovascular gene delivery via therapeutic ultrasound. J. Am. Coll. Cardiol 2001;37:1975–1980. [PubMed: 11401141]

Ammi AY, Mamou J, Wang GI, Cleveland RO, Bridal SL, O'Brien WD Jr. Determining thresholds for contrast agent collapse. Proceedings of the 2004 IEEE Ultrasonics Symposium 2004:308–309.

Ammi AY, Cleveland RO, Mamou J, Wang GI, Bridal SL, O'Brien WD Jr. Ultrasonic contrast agent shell rupture detected by inertial cavitation and rebound signals. IEEE Trans. Ultrasonics Ferroelectrics Frequency Control 2006;53:126–136.

Anderson, L. Bioeffects of 50/60 Hz Fields. In: Greene, MW., editor. Non-Ionizing Radiation: Proceedings of the Second International Non-Ionizing Radiation Workshop. Canadian Radiation Protection Association; Vancouver, BC: 1992. p. 333-352.

Apfel RE. Acoustic cavitation prediction. J. Acoust. Soc. Am 1981a;69:1624–1633.

Apfel, RE. Acoustic cavitation. In: Edmonds, PD., editor. Ultrasonics: Methods of Experimental Physics Series. 356. Academic Press; New York, NY: 1981b.

Apfel RE. Acoustic cavitation: a possible consequence of biomedical uses of ultrasound. Br. J. Cancer 1982;45(Suppl):140–146. [PubMed: 7059457]

Apfel RE. Possibility of microcavitation from diagnostic ultrasound. IEEE Trans. Ultrasonics Ferroelectrics Frequency Control 1986;33:139–142.

Apfel RE, Holland CK. Gauging the likelihood of cavitation from short-pulse, low-duty cycle diagnostic ultrasound. Ultrasound Med. Biol 1991;17:179–185. [PubMed: 2053214]

Arulkumaran S, Talbert DG, Nyman M, Westgren M, Hsu TS, Ratman SS. Audible in utero sound from ultrasound scanner. Lancet 1991;338:704–705. [PubMed: 1679509]

Arulkumaran S, Talbert DG, Nyman M, Westgren M, Hsu TS, Ratman SS. Audible in utero sound caused by the ultrasonic radiation force rom a real-time scanner. J. Obstet. Gynaecol. Res 1996;22:523–527. [PubMed: 9037941]

Bacon DR. Characteristics of a PVDF membrane hydrophone for use in the range 1–100 MHz. IEEE Trans. Sonics Ultrasonics 1982;SU-29:18–25.

Baggs R, Penney DP, Cox C, Child SZ, Raeman CH, Dalecki D, Carstensen EL. Thresholds for ultrasonically induced lung hemorrhage in neonatal swine. Ultrasound Med. Biol 1996;22:119–128. [PubMed: 8928309]

Bao S, Thrall BD, Miller DL. Transfection of a reporter plasmid into cultured cells by sonoporation in vitro. Ultrasound Med. Biol 1997;23:953–959. [PubMed: 9300999]

Baum G. The effect of ultrasonic radiation upon the eye and ocular adnexa. Am. J. Ophthalmol 1956;42:670–696.

BEIR. The Effects on Populations of Exposure to Low Levels of Ionizing Radiation. National Academy of Sciences—National Research Council; Washington, DC: 1972.

BEIR. Health Risks from Exposure to Low Levels of Ionizing Radiation: BEIR VII Phase 2. The National Academies Press; Washington, DC: 2005.

Bercoff J, Tanter M, Fink M. Supersonic shear imaging: a new technique for soft tissue elasticity mapping. IEEE Trans. Ultrasonics Ferroelectrics Frequency Control 2004;51:396–409.

Bernhardt, J. Bioeffects of radiofrequency fields. In: Greene, MW., editor. Non-Ionizing Radiation: Proceedings of the Second International Non-Ionizing Radiation Workshop. Canadian Radiation Protection Association; Vancouver, BC: 1992. p. 32-58.

Beyer, RT. Nonlinear Acoustics. Acoustical Society of America. American Institute of Physics; Woodbury, NY: 1997.

Blackstock, DT. Fundamentals of Physical Acoustics. Wiley: New York, NY: 2000.

Borrelli MJ, Thompson LL, Cain CA, Dewey WC. Time-temperature analysis of cell killing of BHK cells heated at temperatures in the range of 43.5–57 °C. Int. J. Radiat. Oncol. Biol. Phys 1990;19:389–399. [PubMed: 2394618]

Brain KR. Investigations of piezo-electric effects with dielectrics. Proc. Phys. Soc. (London) 1924;36:81–93.

Brayman AA, Miller MW. Sonolysis of Albunex-supplemented, 40% hematocrit human erythrocytes by pulsed 1-MHz ultrasound: pulse number, pulse duration and exposure vessel rotation dependence. Ultrasound Med. Biol 1999;25:307–314. [PubMed: 10320320]

Brayman AA, Coppage ML, Vaidya S, Miller MW. Transient poration and cell surface receptor removal from human lymphocytes in vitro by 1-MHz ultrasound. Ultrasound Med. Biol 1999a;25:999–1008. [PubMed: 10461730]

Brayman AA, Lizotte LM, Miller MW. Erosion of artificial endothelia in vitro by pulsed ultrasound: acoustic pressure, frequency, membrane orientation and microbubble contrast agent dependence. Ultrasound Med. Biol 1999b;25:1305–1320. [PubMed: 10576273]

Breazeale MA, Dunn F. Comparison of methods for absolute calibration of ultrasonic fields. J. Acoust. Soc. Am 1974;55:671–672.

Carson PL, Rubin JN, Chiang EH. Fetal depth and ultrasound path lengths through overlying tissues. Ultrasound Med. Biol 1989;15:629–639. [PubMed: 2683290]

Cavicchi TJ, O'Brien WD Jr. Heat generated by ultrasound in an absorbing medium. J. Acoust. Soc. Am 1984;70:1244–1245. [PubMed: 6501707]

Cavicchi TJ, O'Brien WD Jr. Heating distribution color graphics for homogeneous lossy spheres irradiated with plane wave ultrasound. IEEE Trans. Sonics Ultrasonics 1985;SU-32:17–25.

CGPM. 1975The gray was adopted as the SI unit of absorbed dose by the 15th CGPM (Conférence Générale des Poids et Mesures) in 1975 (Resolution 9)

CGPM. 1976The sievert was adopted as the SI unit of dose equivalent by the 16th CGPM (Conférence Générale des Poids et Mesures) in 1976 (Resolution 5)

Chan SK, Frizzell LA. Ultrasonic thresholds for structural changes in the mammalian liver. Proceedings of the 1977 Ultrasonics Symposium 1977:153–156.

Chapman S, Windle J, Xie F, McGrain A, Porter TR. Incidence of cardiac arrhythmias with therapeutic versus diagnostic ultrasound and intravenous microbubbles. J. Ultrasound Med 2005;24:1099–1107. [PubMed: 16040825]

Chavrier F, Chapelon JY. Modeling of high-intensity focused utlrasound-induced lesions in the presence of cavitation bubbles. J. Acoust. Soc. Am 2000;108:432–440. [PubMed: 10923905]

Chen L, Wansapura JP, Heit G, Butts K. Study of laser ablation in the in vivo rabbit brain with MR thermometry. J. Magn. Resonance Imag 2002;16:147–152.

Cheng HLM, Purcell VT, Bilbao JM, Plewes DB. Prediction of subtle thermal histopathological change using a novel analysis of Gd-DTPA kinetics. J. Magn. Resonance Imag 2003;18:585–598.

Child SZ, Hartman CL, Schery LA, Carstensen EL. Lung damage from exposure to pulsed ultrasound. Ultrasound Med. Biol 1990;16:817–825. [PubMed: 2095012]

Church CC. Spontaneous, homogeneous nucleation, inertial cavitation and the safety of diagnostic ultrasound. Ultrasound Med. Biol 2002;28:1349–1364. [PubMed: 12467862]

Church CC. Frequency, pulse length, and the mechanical index. Acoust. Res. Lett. Online (ARLO) 2005;6:162–168.

Coakley, WT.; Nyborg, WL. Cavitation; dynamics of gas bubbles; applications. In: Fry, FJ., editor. Ultrasound: Its Applications in Medicine and Biology. Elsevier; New York, NY: 1978. p. 77-160.

Crile G Jr. Heat as an adjunct to the treatment of cancer, experimental studies. Cleveland Clin. Quart 1961;28:75–89. [PubMed: 13696466]

Curie J, Curie P. Développement par compression de l'électricité polare dans les cristaux hémièdres à faces inclines. Bull. Soc. Minéral. France 1880;3:90–93.and also published in Comptes Rendus 91, 294–295, 383–386

Curley MG. Soft tissue temperature rise caused by scanned, diagnostic ultrasound. IEEE Trans. Ultrasonics Ferroelectrics Frequency Control 1993;40:59–66.

Daft CMW, Siddiqi TA, Fitting DW, Meyer RA, O'Brien WD Jr. In vivo fetal ultrasound exposimetry. IEEE Trans. Ultrasonics Ferroelectrics Frequency Control 1990;37:501–505.

Dalecki D, Keller BB, Raeman CH, Carstensen EL. Effects of ultrasound on the frog heart, I: thresholds for changes in cardiac rhythm and aortic pressure. Ultrasound Med. Biol 1993;19:385–390. [PubMed: 8356782]

Dalecki D, Child SZ, Raeman CH, Carstensen EL. Tactile perception of ultrasound. J. Acoust. Soc. Am 1995;97:3165–3170. [PubMed: 7759656]

Dalecki D, Keller BB, Raeman CH, Carstensen EL. Effects of ultrasound on the frog heart, III: the radiation force mechanism. Ultrasound Med. Biol 1997a;23:275–285. [PubMed: 9140184]

Dalecki D, Raeman CH, Child SZ, Cox C, Francis CW, Meltzer RS, Carstensen EL. Hemolysis in vivo from exposure to pulsed ultrasound. Ultrasound Med. Biol 1997b;23:307–313. [PubMed: 9140187]

Dalecki D, Child SZ, Raeman CH, Cox C, Carstensen EL. Ultrasonically induced lung hemorrhage in young swine. Ultrasound Med. Biol 1997c;23:777–781. [PubMed: 9253826]

Dalecki D, Child SZ, Raeman CH, Cox C, Penney DP, Carstensen EL. Age dependence of ultrasonically induced lung hemorrhage in mice. Ultrasound Med. Biol 1997d;23:767–776. [PubMed: 9253825]

Dalecki D, Rota C, Raeman CH, Child SZ. Premature cardiac contractions produced by ultrasound and microbubble contrast agents in mice. Acoust. Res. Lett. Online (ARLO) 2005;6:221–226.

DeReggi AS, Roth SC, Kenney JM, Edelman S, Harris GR. Piezoelectric polymer probe for ultrasonic applications. J. Acoust. Soc. Am 1981;69:853–859.

Dewey WC. Arrhenius relationships from the molecule and cell to the clinic. Int. J. Hyperthermia 1994;10:457–483. [PubMed: 7963805]

Dewey WC, Hopwood LE, Sapareto SA, Gerweck LE. Cellular responses to combinations of hyperthermia and radiation. Radiology 1977;123:463–474. [PubMed: 322205]

Dewhirst MW, Viglianti BL, Lora-Michiels M, Hanson M, Hoppes PF. Basic principles of thermal dosimetry and thermal thresholds for tissue damage from hyperthermia. Int. J. Hyperthermia 2003;19:267–294. [PubMed: 12745972]

Dickson, JA.; Calderwood, SK. Temperature range and selective sensitivity of tumors to hyperthermia: a critical review. In: Jain, RK.; Gullino, PM., editors. Thermal Characteristics of Tumors: Applications in Detection Treatment. Annals of the New York Academy of Sciences; New York: 1980. p. 180-205.

Didenko YT, McNamara WB III, Suslick KS. Hot spot conditions during cavitation in water. J. Am. Chem. Soc 1999;121:5817–5818.

Duck FA, Starritt HC, ter Haar GR, Lunt MJ. Surface heating of diagnostic ultrasound transducers. Br. J. Radiol 1989;67:1005–1013. [PubMed: 2684324]

Dunn F, Breyer JE. Generation and detection of ultra-high-frequency sound in liquids. J. Acoust. Soc. Am 1962;34:775–778.

Dunn F, Fry FJ. Ultrasonic threshold dosages for the mammalian central nervous system. IEEE Trans. Biomed. Eng 1971;18:253–256. [PubMed: 4997992]

Dunn F, Averbuch AJ, O'Brien WD Jr. A primary method for the determination of ultrasonic intensity with elastic sphere radiometer. Acustica 1977;38:58–61.

Dyson, M.; Brookes, M. Stimulation of bone repair by ultrasound. In: Lerski, A.; Morley, P., editors. Ultrasound '82. Pergamon Press; Elmsford, NY: 1983. p. 61-66.

Ensminger, D. Ultrasonics: Fundamentals, Technology, Applications. second ed.. Marcel Dekker; New York, NY: 1988.

Fatemi M, Greenleaf JF. Ultrasound-stimulated vibro-acoustic spectrography. Science 1998;280:82–85. [PubMed: 9525861]

Fatemi M, Greenleaf JF. Vibro-acoustography: an imaging modality based on ultrasound-stimulated acoustic emission. Proc. Natl. Acad. Sci. USA 1999;96:6603–6608. [PubMed: 10359758]

Fatemi M, Ogburn PL Jr. Greenleaf JF. Fetal stimulation by pulsed diagnostic ultrasound. J. Ultrasound Med 2001;20:883–889. [PubMed: 11503925]

FDA. Center for Devices and Radiological Health. US Food and Drug Administration; Rockville, MD: 1985. 501(k) Guide for measuring and reporting acoustic output of diagnostic ultrasound medical devices.

FDA. Center for Devices and Radiological Health. US Food and Drug Administration; Rockville, MD: 1987. Diagnostic Ultrasound Guidance Update.

FDA. Center for Devices and Radiological Health. US Food and Drug Administration; Rockville, MD: 1993. Revised 510(k) Diagnostic Ultrasound Guidance for 1993.

FDA. Center for Devices and Radiological Health. US Food and Drug Administration; Rockville, MD: 1994. Use of Mechanical Index in Place of Spatial Peak, Pulse Average Intensity in Determining Substantial Equivalence.

FDA. Information for Manufacturers Seeking Marketing Clearance of Diagnostic Ultrasound Systems and Transducers. US Food and Drug Administration; Rockville, MD: 1997.

Fick SE, Breckenridge FR, Tschiegg CE, Eitzen DG. An ultrasonic absolute power transfer standard. NBS J. Res 1984;89:209–212.

Filipczynski L. The absolute method for intensity measurements of liquid-borne ultrasonic pulses with the electrodynamic transducer. Proc. Vibr. Probl 1967;8:21–26.

Flynn, HG. Physics of acoustic cavitation in liquids. In: Mason, WP., editor. Physical Acoustics. lB & 57. Academic Press; New York, NY: 1964.

Flynn HG. Cavitation dynamics, I: a mathematical formulation. J. Acoust. Soc. Am 1975a;57:1379–1396.

Flynn HG. Cavitation dynamics, II: free pulsations and models for cavitation bubbles. J. Acoust. Soc. Am 1975b;58:1160–1170.

Flynn HG. Generation of transient cavities in liquids by microsecond pulses of ultrasound. J. Acoust. Soc. Am 1982;72:1926–1932.

Flynn HG, Church CC. Transient pulsations of small gas bubbles in water. J. Acoust. Soc. Am 1988;84:985–998.

Foster KR, Wiederhold ML. Auditory responses in cats produced by pulsed ultrasound. J. Acoust. Soc. Am 1978;63:1199–1205. [PubMed: 649878]

French LA, Wild JJ, Neal D. Attempts to determine harmful effects of pulsed ultrasonic vibrations. Cancer 1951;4:342–344. [PubMed: 14821928]

Frizzell LA. Threshold dosages for damage to mammalian liver by high intensity focused ultrasound. IEEE Trans. Ultrasonics Ferroelectrics Frequency Control 1988;35:578–581.

Frizzell LA, Chen E, Lee C. Effects of pulsed ultrasound on the mouse neonate: hind limb paralysis and lung hemorrhage. Ultrasound Med. Biol 1994;20:53–63. [PubMed: 8197627]

Frizzell LA, Linke CA, Carstensen EL, Fridd CW. Thresholds for focal ultrasonic lesions in rabbit kidney, liver, and testicle. IEEE Trans. Biomed. Eng 1977;24:393–396. [PubMed: 881212]

Fry WJ. Action of ultrasound on nerve tissue—a review. J. Acoust. Soc. Am 1953;25:1–5.

Fry WJ, Dunn F. Precision calibration of ultrasonic fields by thermoelectric probes. IRE National Convention Record, Part 9, pp. 39–42. Also published in IRE Trans. Ultrasonics Eng 1957;UE-5:59–65.

Fry WJ, Fry RB. Temperature changes produced in tissue during ultrasonic irradiation. J. Acoust. Soc. Am 1953;25:6–11.

Fry WJ, Fry RB. Determination of absolute sound levels and acoustic absorption coefficients by thermocouple probes—theory. J. Acoust. Soc. Am 1954a;26:296–310.

Fry WJ, Fry RB. Determination of absolute sound levels and acoustic absorption coefficients by thermocouple probes—experiment. J. Acoust. Soc. Am 1954b;26:311–317.

Fry WJ, Wulff WJ, Tucker D,FJ, Fry FJ. Physical factors involved in ultrasonically induced changes in living systems, I: identification of non-temperature effects. J. Acoust. Soc. Am 1950;22:867–876.

Fry WJ, Tucker D, Fry FJ, Wulff WJ. Physical factors involved in ultrasonically induced changes in living systems, II: amplitude duration relations and the effect of hydrostatic pressure for nerve tissue. J. Acoust. Soc. Am 1951;23:364–368.

Fry WJ, Barnard JW, Fry FJ, Krumins RF, Brennan JF. Ultrasonic lesions in the mammalian central nervous system. Science 1955;122:517–518. [PubMed: 13255886]

Fry FJ, Kossoff G, Eggleton RC, Dunn F. Threshold ultrasonic dosages for structural changes in mammalian brain. J. Acoust. Soc. Am 1970;48:1413–1417. [PubMed: 5489906]

Fukada E. Piezoelectricity in polymers and biological materials. Ultrasonics 1968;6:229–234. [PubMed: 5717476]

Gavrilov LR. Use of focused ultrasound for stimulation of nerve structure. Ultrasonics 1984;22:132–138. [PubMed: 6372189]

Gavrilov LR, Gershuni GV, Ilyinski OB, Tsirulnikov EM, Shchekanov EE. A study of reception with the use of focused ultrasound, I: effects on the skin and deep receptor structures in man. Brain Res 1977a;135:265–277. [PubMed: 922476]

Gavrilov LR, Gershuni GV, Ilyinski OB, Tsirulnikov EM, Shchekanov EE. A study of reception with the use of focused ultrasound, II: effects on the animal receptor structures. Brain Res 1977b; 135:279–285. [PubMed: 922477]

Gilmore, FR. The Growth or Collapse of A Spherical Bubble in A Viscous Compressible Liquid. California Institute of Technology; Pasadena, California: 1952.

Goss SA. Sister chromatid exchange and ultrasound. J. Ultrasound Med 1984;3:463–470. [PubMed: 6387170]

Grandolfo, M. Electromagnetic field dosimetry. In: Greene, MW., editor. Non-Ionizing Radiation: Proceedings of the Second International Non-Ionizing Radiation Workshop. Canadian Radiation Protection Association; Vancouver, BC: 1992. p. 76-95.

Greenleaf WJ, Bolander ME, Sarkar G, Goldring MB, Greenleaf JF. Artificial cavitaiton nuclei significantly enhance acoustically induced cell transfection. Ultrasound Med. Biol 1998;24:587–595. [PubMed: 9651968]

Guzman HR, Nguyen DX, Sohail K, Prausnitz MR. Ultrasound-mediated disruption of cell membranes, I: quantification of molecular uptake and cell viability. J. Acoust. Soc. Am 2001;110:588–596. [PubMed: 11508983]

Guzman HR, Nguyen DX, McNamara A, Prausnitz MR. Equilibrium loading of cells with macromolecules by ultrasound: effects of molecular size and acoustic energy. J. Pharm. Sci 2002;91:1693–1701. [PubMed: 12115831]

Hall, DE. Basic Acoustics. Harper & Row; New York, NY: 1987.

Harris GR. Sensitivity considerations for PVDF hydrophones using the spot-poled membrane design. IEEE Trans. Sonics Ultrasonics 1982;SU-29:370–377.

Harris, GR. Ultrasound Safety Standards. In: Greene, MW., editor. Non-Ionizing Radiation: Proceedings of the Second International Non-Ionizing Radiation Workshop. Canadian Radiation Protection Association; Vancouver, BC: 1992. p. 209-224.

Harrison GH, Balcer-Kubiczek E, Gutierrez PL. In vitro mechanisms of chemopotentiation by tone-burst ultrasound. Ultrasound Med. Biol 1996;22:355–362. [PubMed: 8783468]

Hartman CL, Child SZ, Penney DP, Carstensen EL. Ultrasonic heating of lung tissue. J. Acoust. Soc. Am 1992;91:513–516. [PubMed: 1737892]

Harvey EN. Biological aspects of ultrasonic waves: a general survey. Biol. Bull 1930;59:306–325.

Henle, KJ. Arrhenius analysis of thermal responses. In: Strom, FK., editor. Hyperthermia in Cancer Therapy. G.K. Hall Medical Publishers; Boston, MA: 1983. p. 47-53.

Herman BA, Harris GR. Response to “An extended commentary on ‘Models and regulatory considerations for transient temperature rise during diagnostic ultrasound pulses’ by Herman and Harris, 2002” by Miller and Dewey, 2003. Ultrasound Med. Biol 2003;29:1661–1662.

Herrick JF. Temperatures produced in tissues by ultrasound: experimental study using various techniques. J. Acoust. Soc. Am 1953;25:12–16.

Hilgenfeldt S, Lohse D, Zomack M. Response of bubbles to diagnostic ultrasound: a unifying theoretical approach. Eur. Phys. J. B 1998;4:247–255.

Hilgenfeldt S, Lohse D, Zomack M. Sound scattering and localized heat deposition of pulse-driven microbubbles. J. Acoust. Soc. Am 2000;107:3530–3539. [PubMed: 10875397]

Hill CR. Medical ultrasound: an historical review. Br. J. Radiol 1973;46:899–903. [PubMed: 4585016]

Hille, B. Ion Channels of Excitable Membranes. Sinauer Associates, Inc.; Sunderland, MA: 2001.

Hoff, L. Acoustic Characterization of Contrast Agents for Medical Ultrasound Imaging. Kluwer Academic Publishers; Dordrecht, Netherlands: 2001.

Holland CK, Apfel RE. An improved theory for the prediction of microcavitation thresholds. IEEE Trans. Ultrasonics Ferroelectrics Frequency Control 1989;36:204–208.

Holland CK, Deng CX, Apfel RE, Alderman JL, Fenandez LA, Taylor KJW. Direct evidence of cavitation in vivo from diagnostic ultrasound. Ultrasound Med. Biol 1996;22:917–925. [PubMed: 8923710]

Holt RG, Roy RA. Measurements of bubble-enhanced heating from focused, MHz-frequency ultrasound in a tissue-mimicking material. Ultrasound Med. Biol 2001;27:1399–1412. [PubMed: 11731053]

Hornback, NB. Hyperthermia and Cancer: Human Clinical Trial Experience. I and II. CRC Press; Boca Raton, FL: 1984.

Hueter TF, Ballantine HT Jr. Cotter WC. Production of lesions in the central nervous system with focused ultrasound: a study of dosage factors. J. Acoust. Soc. Am 1956;28:192–201.

Hunt, FV. Electroacoustics: The Analysis of Transduction, and its Historical Background. Acoustical Society of America; New York: 1982.

Hwang JH, Brayman AA, Reidy MA, Matula TJ, Kimmey MB, Crum LA. Vascular effects induced by combined 1-MHz ultrasound and microbubble contrast agent treatments in vivo. Ultrasound Med. Biol 2005;31:553–564. [PubMed: 15831334]

Hynynen K, McDannold N, Martin H, Jolesz FA, Vykhodtseva N. The threshold for brain damage in rabbits induced by bursts of ultrasound in the presence of an ultrasound contrast agent (Optison). Ultrasound Med. Biol 2003;29:473–481. [PubMed: 12706199]

ICRU. Radiation Quantities and Units. International Commission on Radiation Units and Measurements; Washington, DC: 1971. Report 19

IEEE. Institute of Electrical and Electronics Engineers. New York, NY: 1990. IEEE Guide for Medical Ultrasound Field Parameter Measurements. IEEE Std. 790-1989

Johnston RL, Dunn F. Ultrasonic absorbed dose, dose rate, and produced lesion volume. Ultrasonics 1976;14:153–155. [PubMed: 936334]

Kawai H. The piezoelectricity of poly (vinylidene fluoride). Jpn. J. Appl. Phys 1969;8:975–976.

Kayhani K, Guzman HR, Parsons A, Lewis TN, Prausnitz MR. Intracellular drug delivery using low-frequency ultrasound: quantification of molecular uptake and cell viability. Pharm. Res 2001;18:1514–1520. [PubMed: 11758757]

Keller JB, Miksis MJ. Bubble oscillations of large amplitude. J. Acoust. Soc. Am 1980;68:628–633.

Kelly E. Ultrasound in Biology and Medicine. 1957Publication No. 3. American

Kelly, E., editor. Ultrasonic Energy: Biological Investigations and Medical Applications. University of Illinois Press; Urbana, IL: 1965.

Killam AL, Greener Y, McFerran BA, Maniquis J, Bloom A, Widder KJ, Dittrich HC. Lack of bioeffects of ultrasound energy after intravenous administration of FS069 (Optison) in the anesthetized rabbit. J. Ultrasound Med 1998;17:349–356. [PubMed: 9623471]

Kinsler, LE.; Frey, AR.; Coopens, AB.; Sanders, JV. Fundamentals of Acoustics. third ed.. Wiley; New York, NY: 1982.

Kobayashi N, Yasu T, Yamada S, Kudo N, Kuroki M, Kawakami M, Miyatake K, Saito M. Endothelial cell injury in venule and capillary induced by contrast ultrasonography. Ultrasound Med. Biol 2002;28:949–956. [PubMed: 12208339]

Kobayashi N, Yasu T, Yamada S, Kudo N, Kuroki M, Miyatake K, Kawakami M, Saito M. Influence of contrast ultrasonography with perflutren lipid microspheres on microvessel injury. Circ. J 2003;67:630–636. [PubMed: 12845189]

Kossoff G. Balance technique for the measurement of very low ultrasonic power outputs. J. Acoust. Soc. Am 1965;38:880–881.

Kremkau, FW. Ultrasonic detection of cavitation at catheter tips. The University of Rochester; Rochester, NY: 1969. MS Thesis

Kremkau FW. Cancer therapy with ultrasound: a historical review. J. Clin. Ultrasound 1979;7:287–300. [PubMed: 112118]

Kremkau F, Gramiak R, Carstensen E, Shah P, Kramer D. Ultrasonic detection of cavitation at catheter tips. Am. J. Roentgenol. Radium Ther.—Nucl. Med 1970;110:177–183.

Langevin, P. French Patent No. 505,703. 1917. (filed September 17, 1917; issued August 5, 1920)

Lawrie A, Brisken AF, Francis SE, Cumberland DC, Crossman DC, Newman CM. Microbubble-enhanced ultrasound for vascular gene delivery. Gene Ther 2000;7:2023–2027. [PubMed: 11175314]

Lehmann JF. The biophysical mode of action of biologic and therapeutic ultrasonic reactions. J. Acoust. Soc. Am 1953;25:17–25.

Leighton, TG. The Acoustic Bubble. Academic Press; New York: 1994.

Lele PP. Hazzard DG, Litz ML. Thresholds and mechanisms of ultrasonic damage to “organized” animal tissues. Symposium on Biological Effects and Characterizations of Ultrasound Sources. US Department of Health, Education, and Welfare HEW Publication (FDA) 78-8048 1977:224–239.

Lele, PP. Physical Aspects and Clinical Studies With Ultrasonic Hyperthermia. In: Strom, FK., editor. Hyperthermia in Cancer Therapy. G.K. Hall Medical Publishers; Boston, MA: 1983. p. 333-367.

Leonowich, J. Measurements of radio frequency fields. In: Greene, MW., editor. Non-Ionizing Radiation: Proceedings of the Second International Non-Ionizing Radiation Workshop. Canadian Radiation Protection Association; Vancouver, BC: 1992. p. 96-124.

Lerner RM, Carstensen EL, Dunn F. Frequency dependence of thresholds for ultrasonic production of thermal lesions in tissue. J. Acoust. Soc. Am 1973;54:504–506. [PubMed: 4759016]

Lewin PA. Miniature piezoelectric polymer ultrasonic hydrophone probes. Ultrasonics 1981;19:213–216.

Lewin, PA.; Schafer, MA. Ultrasound: Measurements and instrumentation. In: Greene, MW., editor. Non-Ionizing Radiation: Proceedings of the Second International Non-Ionizing Radiation Workshop. Canadian Radiation Protection Association; Vancouver, BC: 1992. p. 189-208.

Liebeskind D, Bases R, Mendex F, Elequin F, Koenigsberg M. Sister chromatid exchanges in human lymphocytes after exposure to diagnostic ultrasound. Science 1979;205:1273–1275. [PubMed: 472742]

Lizzi FL, Coleman DJ, Driller J, Franzen LA, Jakobiec FA. Experimental, ultrasonically induced lesions in the retina, choroid, and sclera. Invest. Ophthalmol. Vis. Sci 1978;17:350–360. [PubMed: 640782]

Lizzi FL, Coleman DJ, Diller J, Ostromogilsky M, Chang S, Greenall P. Ultrasonic hyperthermia for ophthalmic therapy. IEEE Trans. Sonics Ultrasonics 1984;SU-31:473–481.

Lubbers J, Hekkenberg RT, Bezemer RA. Time to threshold (TT), a safety parameter for heating by diagnostic ultrasound. Ultrasound Med. Biol 2003;29:755–764. [PubMed: 12754075]

Lyng H, Monge OR, Bohler PJ, Rofstad EK. Relationships between thermal dose and heat-induced tissue and vascular damage after thermoradiotherapy of locally advanced breast carcinoma. Int. J. Hyperthermia 1991;7:403–415. [PubMed: 1919137]

Lynn JG, Putman TJ. Histology of cerebral lesions produced by focused ultrasound. Am. J. Pathol 1944;20:637–649.

Lynn JG, Zwemer RL, Chick AJ, Miller AF. A new method for the generation and use of focused ultrasound in experimental biology. J. Gen. Physiol 1942;26:179–193.

Macintosh IJC, Davey DA. Chromosome aberrations induced by an ultrasonic fetal pulse detector. Br. Med. J 1970;4:92–93. [PubMed: 5471776]

Macintosh IJC, Davey DA. Relationship between intensity of ultrasound and induction of chromosome aberrations. Br. J. Radiol 1972;44:320–327. [PubMed: 5023491]

Macintosh IJC, Brown RC, Coakley WT. Ultrasound and in vitro chromosome aberrations. Br. J. Radiol 1975;48:230–232. [PubMed: 47775]

Magee TR, Davies AH. Auditory phenomena during transcranial Doppler insonation of the basilar artery. J. Ultrasound Med 1993;12:747–750. [PubMed: 8301715]

Matsumoto Y, Watanabe M. Nonlinear oscillation of gas bubbles with internal phenomena. Jpn. Soc. Mech. Eng. Int. J 1989;32:157–162.

McDannold NJ, King RL, Jolesz FA, Hynynen KH. Usefulness of MR imaging-derived thermometry and dosimetry in determining the threshold for tissue damage induced by thermal surgery in rabbits. Radiology 2000;216:517–523. [PubMed: 10924580]

McDannold N, Vykhodtseva N, Jolesz FA, Hynynen K. MRI investigation of the threshold for thermally induced blood-brain barrier disruption and brain tissue damage in the rabbit brain. Magn. Resonance Med 2004;51:913–923.

McNeil PL. Incorporation of macromolecules into living cells. Methods Cell Biol 1989;29:153–173. [PubMed: 2643758]

Merritt CRB. Ultrasound safety: what are the issues? Radiology 1989;173:304–306. [PubMed: 2678243]

Miller AP, Nanda NC. Contrast echocardiography: new agents. Ultrasound Med. Biol 2004;30:425–434. [PubMed: 15121243]

Miller DL, Bao S. The relationship of scattered subharmonic, 3.3-MHz fundamental and second harmonic signals to damage of monolayer cells by ultrasonically activated Albunex. J. Acoust. Soc. Am 1998;103:1183–1189. [PubMed: 9479770]

Miller DL, Gies RA. Enhancement of ultrasonically-induced hemolysis by perfluorocarbon-based compared to air-based echo-contrast agents. Ultrasound Med. Biol 1998a;24:285–292. [PubMed: 9550187]

Miller DL, Gies RA. Gas-body-based contrast agent enhances vascular bioeffects of 1.09 MHz ultrasound on mouse intestine. Ultrasound Med. Biol 1998b;24:1201–1208. [PubMed: 9833589]

Miller DL, Gies RA. The influence of ultrasound frequency and gas-body composition on the contrast agent-medicated enhancement of vascular bioeffects in mouse intestine. Ultrasound Med. Biol 2000;26:307–313. [PubMed: 10722920]

Miller DL, Song J. Tumor growth reduction and DNA transfer by cavitation-enhanced high-intensity focused ultrasound in vivo. Ultrasound Med. Biol 2003;29:887–893. [PubMed: 12837504]

Miller DL, Quddus J. Sonoporation of monolayer cells by diagnostic ultrasound activation of contrast-agent gas bodies. Ultrasound Med. Biol 2000a;26:661–667. [PubMed: 10856630]

Miller DL, Quddus J. Diagnostic ultrasound activation of contrast agent gas bodies induces capillary rupture in mice. Proc. Natl. Acad. Sci. USA 2000b;97:10179–10184. [PubMed: 10954753]

Miller DL, Gies RA, Chrisler WB. Ultrasonically induced hemolysis at high cell and gas body concentrations in a thin-disc exposure chamber. Ultrasound Med. Biol 1997;23:625–633. [PubMed: 9232772]

Miller DL, Bao S, Gies RA, Thrall BD. Ultrasonic enhancement of gene transfection in murine melanoma tumors. Ultrasound Med. Biol 1999;25:1425–1430. [PubMed: 10626630]

Miller DL, Dou C, Song J. DNA transfer and cell killing in epidermoid cells by diagnostic ultrasound activation of contrast agent gas bodies in vitro. Ultrasound Med. Biol 2003;29:601–607. [PubMed: 12749930]

Miller MW, Dewey WC. An extended commentary on “Models and regulatory considerations for transient temperature rise during diagnostic ultrasound pulses” by Herman and Harris (2002). Ultrasound Med. Biol 2003;29:1653–1659. [PubMed: 14654160]

Miller MW, Ziskin MC. Biological consequences of hyperthermia. Ultrasound Med. Biol 1989;15:707–722. [PubMed: 2694557]

Morse, PM.; Ingard, KU. Theoretical Acoustics. Mc-Graw Hill; New York, NY: 1968.

Mukherjee D, Wong J, Griffin B. Ten-fold augmentation of endothelial uptake of vascular endothelial growth factor with ultrasound after systemic administration. J. Am. Coll. Cardiol 2000;35:1678–1686. [PubMed: 10807476]

NCRP. Biological effects of ultrasound: mechanisms and clinical implications. National Council on Radiation Protection and Measurement; Bethesda, MD: 1983. NCRP Report No. 74

NCRP. Implementation of the Principle of as Low as Reasonably Achievable (ALARA) for Medical and Dental Personnel. National Council on Radiation Protection and Measurements (NCRP); Bethesda, MD: 1990. Report No. 107

NCRP. Exposure Criteria for Medical Diagnostic Ultrasound, I: Criteria Based on Thermal Mechanisms. National Council on Radiation Protection and Measurements; Bethesda, MD: 1992. Report No. 113

NCRP. Exposure Criteria for Medical Diagnostic Ultrasound, II: Criteria Based on all Known Mechanisms. National Council on Radiation Protection and Measurements; Bethesda, MD: 2002. Report No. 140

Newell JA. A radiation pressure balance for the absolute measurement of ultrasonic power. Phys. Med. Biol 1963;8:215–221. [PubMed: 13938247]

Nightingale KR, Kornguth PJ, Walker WF, McDermott BA, Trahey GE. A novel ultrasonic technique for differentiating cysts from solid lesions: preliminary results in the breast. Ultrasound Med. Biol 1995;21:745–751. [PubMed: 8571462]

Nightingale KR, Palmeri ML, Nightingale RW, Trahey GE. On the feasibility of remote palpation using acoustic radiation force. J. Acoust. Soc. Am 2001;110:625–634. [PubMed: 11508987]

NIH. Report of an NIH Consensus Development Conference. US Government Printing Office; Washington, DC: 1984. Diagnostic Ultrasound Imaging in Pregnancy. NIH Publication No. 84-667

Nyborg WL. Acoustic streaming due to attenuated plane waves. J. Acoust. Soc. Am 1953;25:68–75.

Nyborg, WL. Acoustic streaming. In: Mason, WP., editor. Physical Acoustics. 2B. Academic Press; New York, NY: 1965. p. 265-331.

Nyborg, WL. Intermediate Biophysical Mechanics. Cummings Publishing Co.; Menlo Park, CA: 1975.

Nyborg, WL. Physical principles of ultrasound. In: Fry, FJ., editor. Ultrasound: Its Applications in Medicine and Biology. Elsevier; New York, NY: 1978. p. 1-76.

Nyborg WL. Heat generation by ultrasound in a relaxing medium. J. Acoust. Soc. Am 1981;70:310–312.

Nyborg WL, O'Brien WD Jr. An alternative simple formula for temperature estimate. J. Ultrasound Med 1989;8:653–654. [PubMed: 2687498]

Nyborg WL, Steele RB. Temperature elevation in a beam of ultrasound. Ultrasound Med. Biol 1983;9:611–620. [PubMed: 6670146]

O'Brien, WD, Jr.. Ultrasonic dosimetry. In: Fry, FJ., editor. Ultrasound: Its Applications in Medicine and Biology. Elsevier; New York, NY: 1978. p. 343-391.

O'Brien WD Jr. Safety of ultrasound with selected emphasis for obstetrics. Semin. Ultrasound 1984;5:105–120.

O'Brien, WD, Jr.. Echocardiography: A Review of Cardiovascular Ultrasound. 3. Futura Publishing Co.; New York, NY: 1986. Biological effects of ultrasound: rationale for the measurement of selected ultrasonic output quantities; p. 165-179.

O'Brien, WD, Jr.. Ultrasound bioeffects related to obstetric sonography. In: Fleischer, AC., et al., editors. The Principles and Practice of Ultrasonography in Obstetrics and Gynecology. fourth ed.. Appleton & Lange; Norwalk, CT: 1991. p. 15-23.

O'Brien, WD, Jr.. Introduction to ultrasound. In: Greene, MW., editor. Non-Ionizing Radiation: Proceedings of the Second International Non-Ionizing Radiation Workshop. Canadian Radiation Protection Association; Vancouver, BC: 1992a. p. 127-150.

O'Brien, WD, Jr.. Ultrasound dosimetry and interaction mechanisms. In: Greene, MW., editor. Non-Ionizing Radiation: Proceedings of the Second International Non-Ionizing Radiation Workshop. Canadian Radiation Protection Association; Vancouver, BC: 1992b. p. 151-172.

O'Brien WD Jr. Assessing the risks for modern diagnostic ultrasound imaging. Jpn. J. Appl. Phys 1998;37:2781–2788.

O'Brien WD Jr. Ellis DS. Evaluation of the soft-tissue thermal index. IEEE Trans. Ultrasonics Ferroelectrics Frequency Control 1999;46:1459–1476.

O'Brien, WD., Jr.; Withrow, TJ. An approach to ultrasonic risk assessment and an examination of selected experimental studies. In: Sanders, RC.; James, AE., Jr., editors. The Principles and Practice of Ultrasonography in Obstetrics and Gynecology. third ed.. Appleton-Century-Crofts; Norwalk, CT: 1985. p. 15-22.

O'Brien WD Jr. Shore ML, Fred RK, Leach WM. On the assessment of risk to ultrasound. Proc. IEEE Ultrasonics Symp 1972:486–490.

O'Brien WD Jr. Frizzell LA, Weigel RM, Zachary JF. Ultrasound-induced lung hemorrhage is not caused by inertial cavitation. J. Acoust. Soc. Am 2000;108:1290–1297. [PubMed: 11008829]

O'Brien WD Jr. Simpson DG, Frizzell LA, Zachary JF. Superthreshold behavior and threshold estimation of ultrasound-induced lung hemorrhage in adult rats: role of beamwidth. IEEE Trans. Ultrasonics Ferroelectrics Frequency Control 2001;48:1695–1705.

O'Brien WD Jr. Abbott JG, Stratmeyer ME, Harris GR, Schafer ME, Siddiqi TA, Merritt CRB, Duck FA, Bendick PB. Acoustic output upper limits: point-counter point, proposition: should upper limits be retained? J. Ultrasound Med 2002;21:1335–1341. [PubMed: 12494975]

O'Brien WD Jr. Simpson DG, Ho M-H, Miller RJ, Frizzell LA, Zachary JF. Superthreshold behavior and threshold estimation of ultrasound-induced lung hemorrhage in pigs: role of age dependency. IEEE Trans. Ultrasonics Ferroelectrics Frequency Control 2003a;50:153–169.

O'Brien WD Jr. Simpson DG, Frizzell LA, Zachary JF. Threshold estimates and superthreshold behavior of ultrasound-induced lung hemorrhage in adult rats: role of pulse duration. Ultrasound Med. Biol 2003b;29:1625–1634. [PubMed: 14654157]

O'Brien WD Jr. Yang Y, Simpson DG. Evaluation of unscanned-mode soft-tissue thermal index for rectangular sources and proposed new indices. Ultrasound Med. Biol 2004a;30:965–972. [PubMed: 15313328]

O'Brien WD Jr. Simpson DG, Frizzell LA, Zachary JF. Effect of contrast agent on the incidence and magnitude of ultrasound-induced lung hemorrhage in rats. Echocardiography 2004b;21:417–422. [PubMed: 15209720]

O'Brien WD Jr. Yang Y, Simpson DG, Frizzell LA, Miller RJ, Blue JP Jr. Zachary JF. Threshold estimation of ultrasound-induced lung hemorrhage in adult rabbits, and comparison of thresholds in mice, rats, rabbits and pigs. Ultrasound Med. Biol 2006;38in press

ODS. Standard for Real-Time Display of Thermal and Mechanical Indices on Diagnostic Ultrasound Equipment. American Institute of Ultrasound in Medicine; Laurel, MD: 1992. and National Electrical Manufacturers Association, Rosslyn, VA

ODS. Standard for the Real-Time Display of Thermal and Mechanical Acoustic Output Indices on Diagnostic Ultrasound Equipment, Rev 1. American Institute of Ultrasound in Medicine; Laurel, MD: 1998. and National Electrical Manufacturers Association, Rosslyn, VA

ODS. Standard for the Real-Time Display of Thermal and Mechanical Acoustic Output Indices on Diagnostic Ultrasound Equipment, Rev 2. American Institute of Ultrasound in Medicine; Laurel, MD: 2004. and National Electrical Manufacturers Association, Rosslyn, VA

Pennes HH. Analysis of tissue and arterial blood temperatures in the resting human forearm. J. Appl. Phys 1948;1:93–122.

Peters RD, Chan E, Trachtenberg J, Jothy S, Kapusta L, Kucharczyk W, Henkelman RM. Magnetic resonance thermometry for predicting thermal damage: an application of interstitial laser coagulation in an in vivo canine prostate model. Magn. Resonance Med 2000;44:873–883.

Pierce, AD. Acoustics: An Introduction to Its Physical Principles and Applications. Mc-Graw Hill; New York, NY: 1981. (A 1989 edition is published by the Acoustical Society of America through the American Institute of Physics, Woodbury, NY)

Poliachik SL, Chandler WL, Mourad PD, Bailey MR, Bloch S, Cleveland RO, Kaczkowski P, Keilman G, Porter T, Crum LA. Effect of high-intensity focused ultrasound on whole blood with and without microbubble contrast agent. Ultrasound Med. Biol 1999;25:991–998. [PubMed: 10461729]

Pond, JB. A Study of the Biological Action of Focussed Mechanical Waves (Focussed Ultrasound). London University; 1968. Ph.D. Thesis

Pond JB. The role of heat in the production of ultrasonic focal lesions. J. Acoust. Soc. Am 1970;47:1607–1611. [PubMed: 5426311]

Preston RC, Bacon DR, Livett AJ, Rajendran K. PVDF membrane hydrophone performance properties and their relevance to the measurement of the acoustic output of medical ultrasonic equipment. J. Phys. E: Sci. Instrum 1983;16:786–796.

Prosperetti A, Lezzi A. Bubble dynamics in a compressible liquid, Part 1. first-order theory. J. Fluid Mech 1986;168:457–478.

Purnell EW, Solollu A, Torchia R, Taner H. Focal chorioretinitis produced by ultrasound. Invest. Ophthalmol 1964;3:657–664. [PubMed: 14238877]

Reid, JM.; Sikov, MR., editors. Interaction of Ultrasound and Biological Tissues. Food and Drug Administration; Rockville, MD: 1972. DHEW Publication (FDA) 73-8008

Raeman CH, Child SZ, Carstensen EL. Timing of exposures in ultrasonic hemorrhage of murine lung. Ultrasound Med. Biol 1993;19:507–512. [PubMed: 8236592]

Raeman CH, Child SZ, Dalecki D, Cox C, Carstensen EL. Exposure-time dependence of the threshold for ultrasonically induced murine lung hemorrhage. Ultrasound Med. Biol 1996;22:139–141. [PubMed: 8928311]

Robinson TC, Lele PP. An analysis of lesion development in the brain and in plastics by high intensity focused ultrasound at low megahertz frequencies. J. Acoust. Soc. Am 1972;51:1333–1351. [PubMed: 5032950]

Rupert CS. Dosimetric concepts in photobiology. Photochem. Photobiol 1974;20:203–212. [PubMed: 4412864]

Sapareto SA, Dewey WC. Thermal dose determination in cancer therapy. Int. J. Radiat. Oncol. Biol. Phys 1984;10:787–800. [PubMed: 6547421]

Schlachetzki F, Holscher T, Koch HJ, Draganski B, May A, Schuierer G, Bogdahn U. Observation on the integrity of the blood-brain barrier after microbubble destruction by diagnostic transcranial color-coded sonography. J. Ultrasound Med 2002;21:419–429. [PubMed: 11934099]

Selawry OX, Goldstein MW, McCormick T. Hyperthermia in tissue-cultured cells of malignant origin. Cancer Res 1957;17:785–791. [PubMed: 13460984]

Siddiqi TA, O'Brien WD Jr. Meyer RA, Sullivan JM, Miodovnik M. In situ exposimetry: The ovarian ultrasound examination. Ultrasound Med. Biol 1991;17:257–263. [PubMed: 1887511]

Simpson DG, Ho M-H, Yang Y, Zhou J, Zachary JF, O'Brien WD. Excess risk thresholds in ultrasound safety studies: Statistical methods for data on occurrence and size of lesions. Ultrasound Med. Biol 2004;30:1289–1295. [PubMed: 15582228]

Sjoberg A, Stable J, Johnson S, Sahl R. Treatment of Meniere's disease by ultrasonic irradiation. Acta Otolaryngol. Suppl 1963;178:171–175.

Skyba DM, Price RJ, Linka AZ, Skalak TC, Kaul S. Direct in vivo visualization of intravascular destruction of microbubbles by ultrasound and its local effects on tissue. Circulation 1998;98:290–293. [PubMed: 9711932]

Sliney, D. Measurements and bioeffects of infrared and visible light. In: Greene, MW., editor. Non-Ionizing Radiation: Proceedings of the Second International Non-Ionizing Radiation Workshop. Canadian Radiation Protection Association; Vancouver, BC: 1992. p. 252-267.

Smith NB, Webb AG, Ellis DS, Wilmes LJ, O'Brien WD Jr. Experimental verification of theoretical in vivo ultrasound heating using cobalt detected magnetic resonance. IEEE Trans. Ultrasonics Ferroelectrics Frequency Control 1995;42:489–491.

Smith, RA. The Calibration of Hydrophones for Use in Medical Ultrasonic Fields—A Review. National Physical Laboratory; Teddington, Middlesex, UK: 1986. NPL Report AC 108

Sokka SD, King R, Hynynen K. MRI-guided bubble enhanced ultrasound heating in in vivo rabbit thigh. Phys. Med. Biol 2003;48:223–241. [PubMed: 12587906]

Stavros, AT.; Dennis, MA. The ultrasound of breast pathology. In: Parker, SH.; Jobe, WE., editors. Percutaneous Breast Biopsy. Raven Press; New York: 1993. p. 111-115.

Stewart, HF.; Stratmeyer, ME., editors. An Overview of Ultrasound: Theory, Measurement, Medical Applications and Biological Effects. US Government Printing Office; Washington, DC: 1982. Health and Human Services Publication (FDA) 82-8190

Suslick, KS. Sonochemistry and Sonoluminescence in Encyclopedia of Physical Science and Technology. third ed.. 17. Academic Press; San Diego: 2001. p. 363-376.

Taylor KJW, Pond JB. A study of the production of hemorrhagic injury and paraplegia in rat spinal cord by pulsed ultrasound of low megahertz frequencies in the context of the safety for clinical usage. Br. J. Radiol 1972;45:343–353. [PubMed: 5023495]

ter Haar, GR. Therapeutic and surgical applications. In: Hill, CR.; Bamber, JC.; ter Haar, GR., editors. Physical Principles of Medical Ultrasonics. second ed.. Wiley; New York: 2004. p. 407-456.

ter Haar, GR.; Duck, FA., editors. British Medical Ultrasound Society. The British Institute of Radiology; London: 2000. The Safe Use of Ultrasound in Medical Diagnosis.

Thomenius KE. Thermal dosimetry models for diagnostic ultrasound. Proceedings of the 1990 Ultrasonics Symposium 1990:1399–1408.

Tsirulnikov EM, Vartanyan IA, Gersuni GV, Rosenblyum AS, Pudov VI, Gavrilov LR. Use of amplitude-modulated focused ultrasound for diagnosis of hearing disorders. Ultrasound Med. Biol 1988;14:277–285. [PubMed: 3046092]

Umemura S, Kawabata K, Sasaki K. In vivo acceleration of ultrasonic tissue heating by microbubble agent. IEEE Trans. Ultrasonics Ferroelectrics Frequency Control 2005;52:1690–1698.

Van der Wouw P, Brauns AC, Bailey SE, Powers JE, Wilde AA. Premature ventricular contractions during triggered imaging with ultrasound contrast. J. Am. Soc. Echocardiogr 2000;13:288–294. [PubMed: 10756246]

van Wamel A, Bouakaz A, Bernard B, ten Cate F, de Jong N. Radionuclide tumour therapy with ultrasound contrast microbubbles. Ultrasonics 2004;42:903–906. [PubMed: 15047404]

Verral, RE.; Sehgal, CM. Sonoluminescence. In: Suslick, KS., editor. Ultrasound: Its Chemical, Physical and Biological Effects. VCH Publishers; New York: 1988. (Chapter 6)

Vykhodtseva N, Sorrentino V, Jolesz FA, Bronson RT, Hynynes K. MRI detection of the thermal effects of focused ultrasound on the brain. Ultrasound Med. Biol 2000;26:871–880. [PubMed: 10942834]

Wall PD, Tucker D, Fry FJ, Mosberg WH. The use of high intensity ultrasound in experimental neurology. J. Acoust. Soc. Am 1953;25:281–285.

Wang C, Chen H, Chen C, Yang K. Treatment of nonunions of long bone fractures with shock waves. Clin. Orthop. Rel. Res 2001;387:95–101.

Wang, GI.; Ammi, AY.; Bridal, SL.; O'Brien, WD, Jr.. A comparison between the modified Herring equation and experimental collapse thresholds; The Annual Meeting of the American Institute of Ultrasound in Medicine; March, 2006; 2006.

Wang SJ, Lewallen DG, Bolander ME, Chao EYS, Ilstrup DM, Greenleaf JF. Low intensity ultrasound treatment increases strength in a rat femoral fracture model. J. Orthop. Res 1994;12:40–47. [PubMed: 8113941]

Ward M, Wu J, Chiu JF. Ultrasound-induced cell lysis and sonoporation enhanced by contrast agents. J. Acoust. Soc. Am 1999;105:2951–2957. [PubMed: 10335644]

Webster WS, Edwards MJ. Hyperthermia and the induction of neural tube defects in mice. Teratology 1984;29:417–425. [PubMed: 6463904]

Weimann LJ, Wu J. Transdermal delivery of poly-l-lysine by sonomacroporation. Ultrasound Med. Biol 2002;28:1173–1180. [PubMed: 12401388]

Weinbaum S, Jiji LM, Lemons DE. Theory and experiment for the effect of vascular microstructure on surface tissue heat transfer—part I: anatomical foundation and model conceptualization. J. Biomech. Eng 1984;106:321–330. [PubMed: 6513527]

Wells PNT, Bullen MA, Follett DH, Freundlich HF, James JA. The dosimetry of small ultrasonic beams. Ultrasonics 1963;1:106–110.

WFUMB. Barnett SB, Kossoff G. WFUMB symposium on safety and standardization in medical ultrasound: Issues and recommendations regarding thermal mechanisms for biological effects of ultrasound. World Federation for Ultrasound in Medicine and Biology. Published in Ultrasound Med. Biol 1992;18:731–814.

WFUMB. Barnett SB. WFUMB symposium on safety of ultrasound in medicine: Conclusions and recommendations on thermal and nonthermal mechanisms for biological effects of ultrasound. World Federation for Ultrasound in Medicine and Biology. Published in Ultrasound Med. Biol 1996;24:S1–S58.

Wible JH Jr. Galen KP, Wojdyla JK, Hughes MS, Klibanov AL, Brandenburger GH. Microbubbles induce renal hemorrhage when exposed to diagnostic ultrasound in anesthetized rats. Ultrasound Med. Biol 2002;28:1535–1546. [PubMed: 12498949]

Wild JJ, Reid JM. The effects of biological tissues on 15-mc pulsed ultrasound. J. Acoust. Soc. Am 1953;25:270–280.

Williams AR, Kubowicz G, Cramer E, Schlief R. The effects of the microbubble suspension SH U 454 (Echovist) on ultrasound-induced cell lysis in a rotating tube exposure system. Echocardiography 1991;8:423–433. [PubMed: 10149264]

Wood RW, Loomis AL. The physical and biological effects of high-frequency sound waves of great intensity. Philos. Mag. (VII) 1927;4:417–436.

Wyber JA, Andrews J, D'Emanuele A. The use of sonication for the efficient delivery of plasmid DNA into cells. Pharm. Res 1997;14:750–756. [PubMed: 9210192]

Yang X, Church CC. Nonlinear dynamics of gas bubbles in viscoelastic media. Acoust. Res. Lett. Online (ARLO) 2005;6:151–156.

Zachary JF, Sempsrott JM, Frizzell LA, Simpson DG, O'Brien WD Jr. Superthreshold behavior and threshold estimation of ultrasound-induced lung hemorrhage in adult mice and rats. IEEE Trans. Ultrasonics Ferroelectrics Frequency Control 2001a;48:581–592.

Zachary JF, Frizzell LA, Norrell KS, Blue JP Jr. Miller RJ, O'Brien WD Jr. Temporal and spatial evaluation of lesion reparative responses following superthreshold exposure of rat lung to pulsed ultrasound. Ultrasound Med. Biol 2001b;27:829–839. [PubMed: 11516543]

Zachary JF, Hartleben SA, Frizzell LA, O'Brien WD Jr. Arrhythmias in rat hearts exposed to pulsed ultrasound after intravenous injection of a contrast agent. J. Ultrasound Med 2002;21:1347–1356. [PubMed: 12494976]

Zachary JF, Blue JP Jr. Miller RJ, Ricconi BJ, Eden JG, O'Brien WD Jr. Lesions of ultrasound-induced lung hemorrhage are not consistent with thermal injury. Ultrasound Med. Biol 2006;38in press

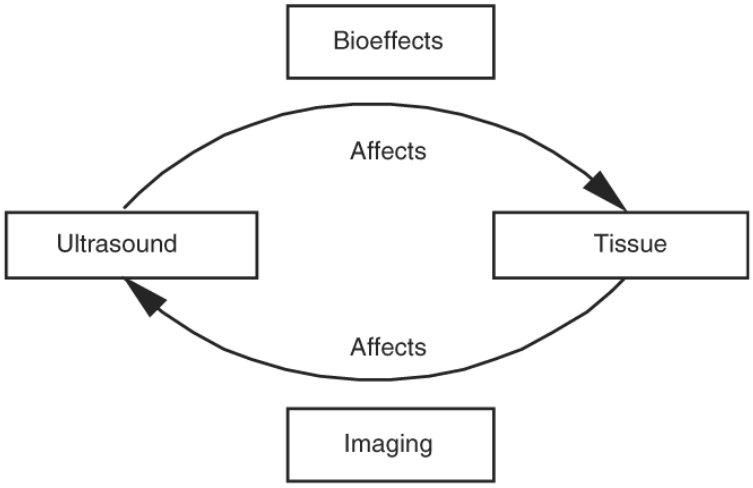

Fig 1.
Schematic diagram of ultrasonic biophysics.

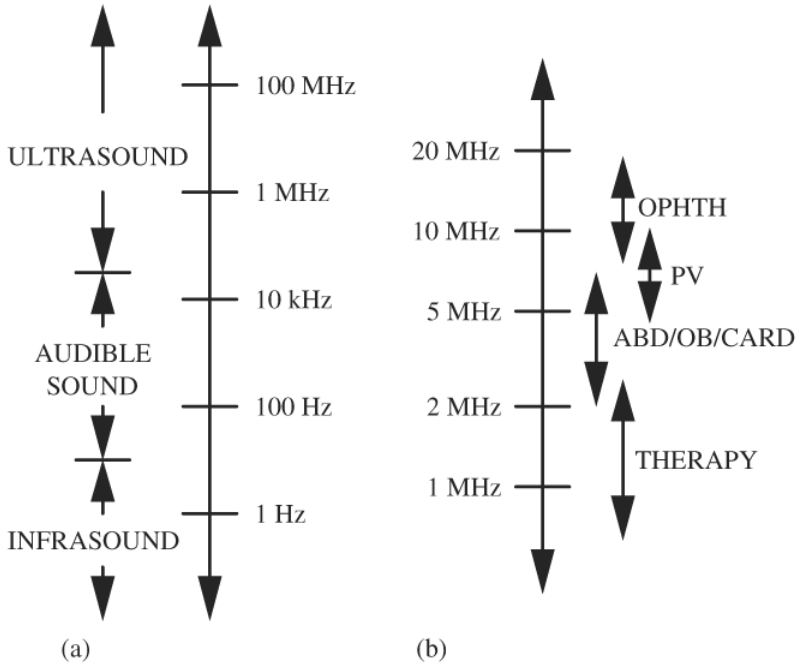

Fig 2.
(a) Acoustic spectrum and (b) medical ultrasound spectrum.

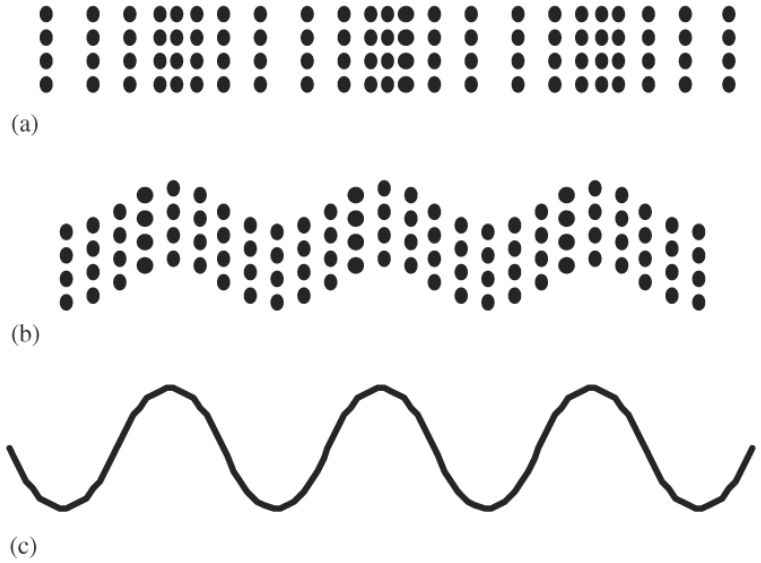

Fig 3.
Representations of longitudinal and shear waves: (a) longitudinal wave representation, (b) shear wave representation and (c) sine wave representation.

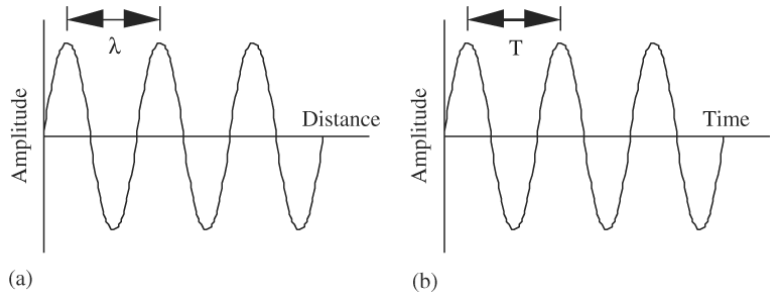

Fig 4.
Schematic representations of an acoustic waveform: (a) amplitude vs. distance and (b) amplitude vs. time.

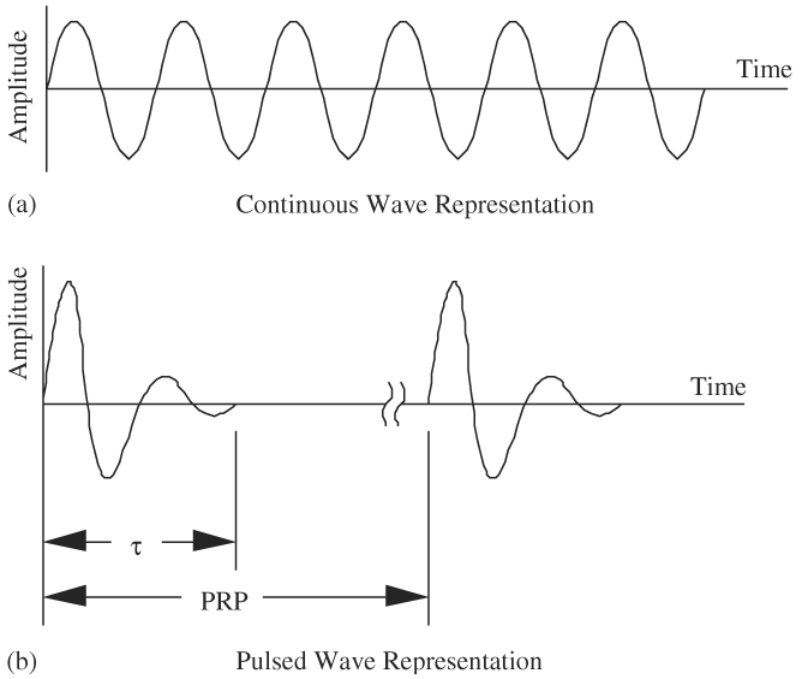

Fig 5.
Schematic representations of continuous wave and pulsed wave ultrasound waveforms: (a) continuous wave representation and (b) pulsed wave representation.

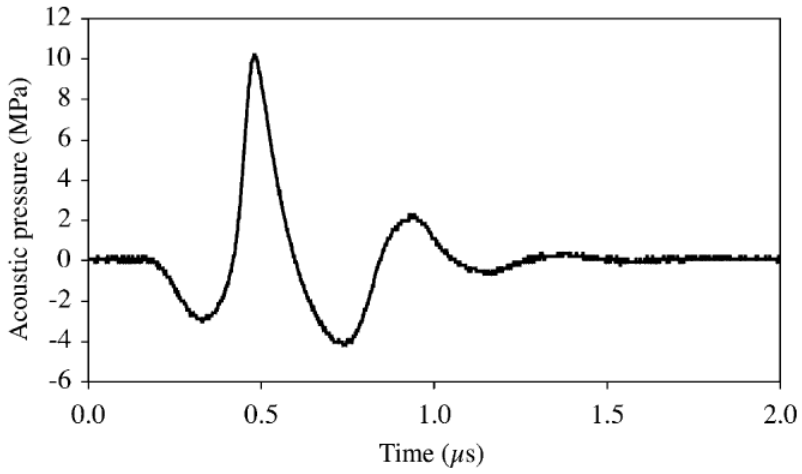

Fig 6.
Measured 2.5-MHz center frequency pulsed wave ultrasound waveform.

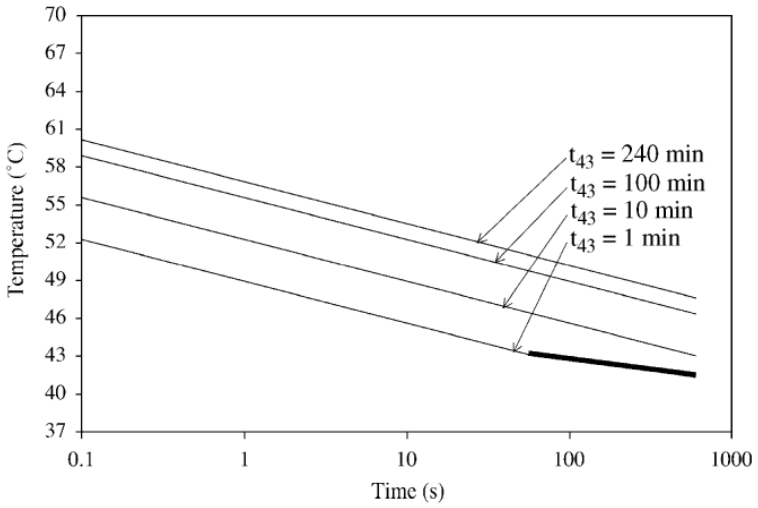

Fig 7.

Temperature–time curves for 4 values of t_{43} (see Eq. (54) for which $R = 0.5$ for $T>43$ °C and $R = 0.25$ for $T\leq 43$ °C). The bolded $t_{43} = 1$ min line shows the lower exposure duration range (applicable to 1 min) of the March 26, 1997 *AIUM Conclusions Regarding Heat* statement (AIUM, 1997).

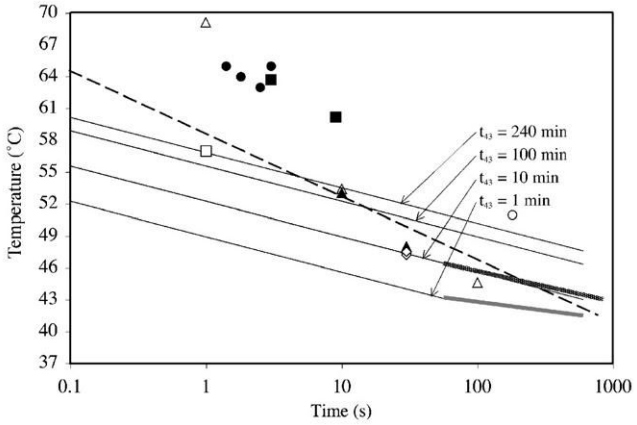

Fig 8.

Temperature–time curves (see Fig. 7) plus the following threshold data: filled-in circle, cat brain; open triangle: extrapolated cat brain; filled-in triangle, rabbit brain; filled-in square, rat brain; open diamond, rabbit muscle; open circle, dog prostate; open square, BHK cells, dashed line, multiple tissue thresholds; shaded line (just above bolded t_{43} = 1 min line), multiple in vitro thresholds. Details listed in Table 9.

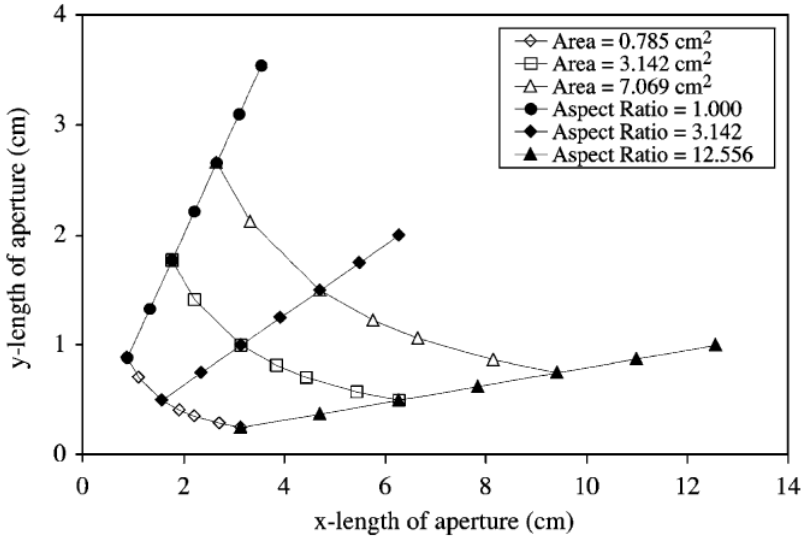

Fig 9.
Dimensions of the 33 rectangular aperture cases investigated.

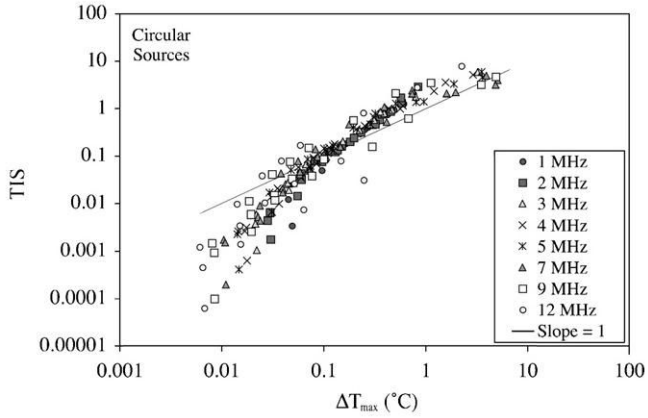

Fig 10.

Paired maximum steady-state temperature increase ΔT_{max} vs. unscanned-mode soft-tissue Thermal Index (TIS) for circular sources grouped by frequency under the condition that the derated (0.3 dB/cm MHz) spatial-peak, temporal-average intensity $I_{SPTA.3}$ is 720 mW/cm^2.

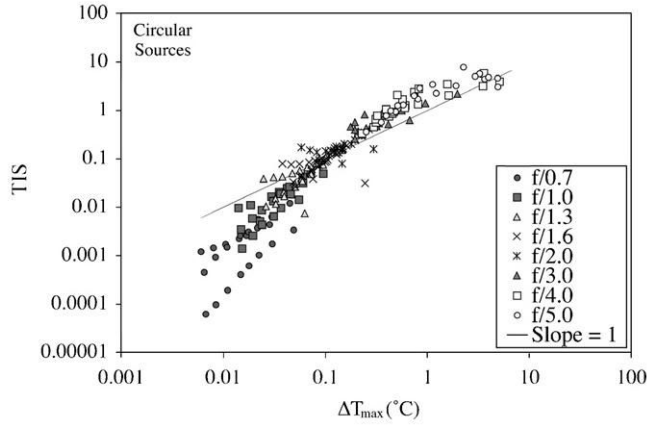

Fig 11.

Paired maximum steady-state temperature increase ΔT_{max} vs. unscanned-mode soft-tissue Thermal Index (TIS) for circular sources grouped by *f*-number under the condition that the derated (0.3 dB/cm MHz) spatial-peak, temporal-average intensity $I_{SPTA.3}$ is 720 mW/cm^2.

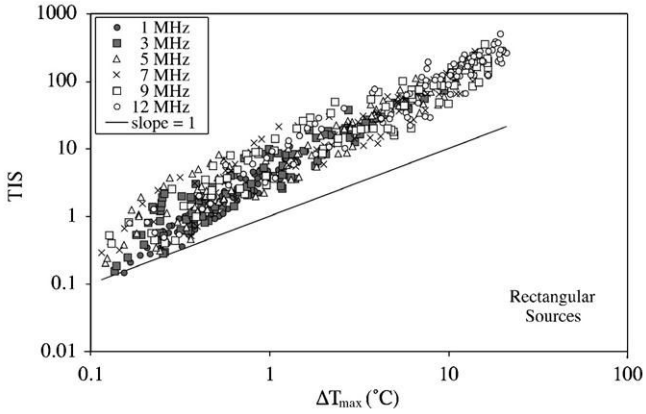

Fig 12.

Paired maximum steady-state temperature increase ΔT_{max} vs. unscanned-mode soft-tissue Thermal Index (TIS) for rectangular sources grouped by frequency under the condition that the derated (0.3 dB/cm MHz) spatial-peak, temporal-average intensity $I_{SPTA.3}$ is 720 mW/cm^2.

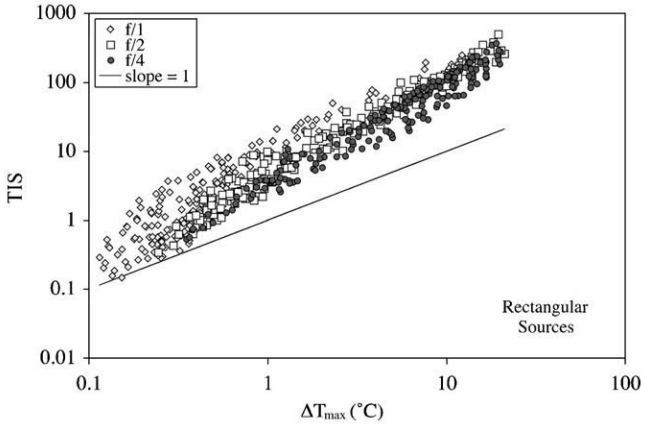

Fig 13.

Paired maximum steady-state temperature increase ΔT_{max} vs. unscanned-mode soft-tissue Thermal Index (TIS) for rectangular sources grouped by *f*-number under the condition that the derated (0.3 dB/cm MHz) spatial-peak, temporal-average intensity $I_{SPTA.3}$ is 720 mW/cm^2.

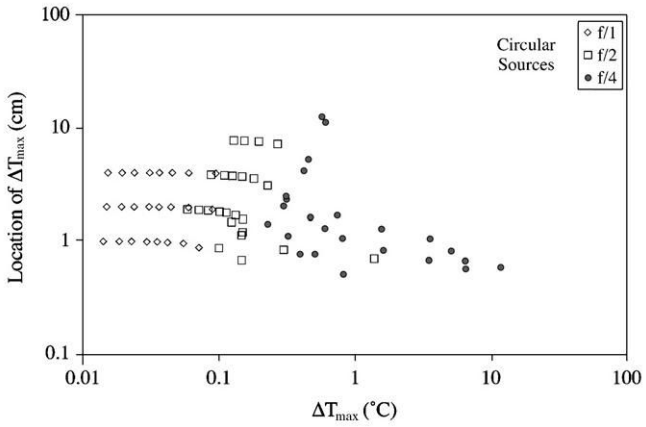

Fig 14.

Paired maximum steady-state temperature increase ΔT_{max} vs. location (axial distance) of ΔT_{max} for circular sources grouped by *f*-number under the condition that the derated (0.3 dB/cm MHz) spatial-peak, temporal-average intensity $I_{SPTA.3}$ is 720 mW/cm^2.

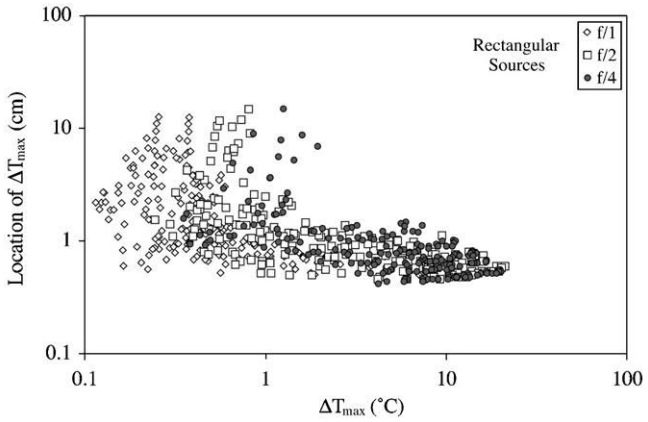

Fig 15.

Paired maximum steady-state temperature increase ΔT_{max} vs. location (axial distance) of ΔT_{max} for rectangular sources grouped by *f*-number under the condition that the derated (0.3 dB/cm MHz) spatial-peak, temporal-average intensity $I_{SPTA.3}$ is 720 mW/cm^2.

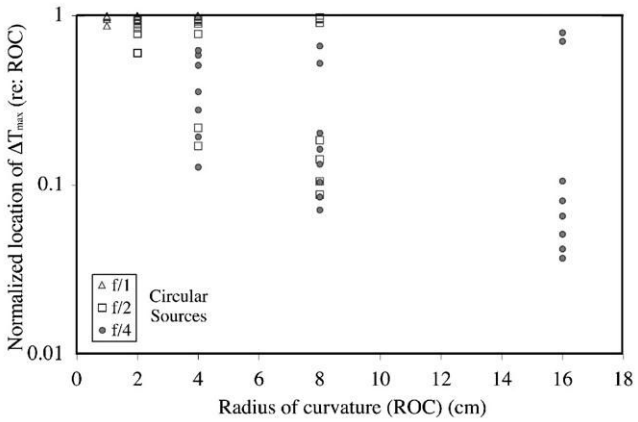

Fig 16.

Paired location of the geometric focus (ROC) vs. normalized location (axial distance) of ΔT_{max} (location of ΔT_{max}/ROC) for circular sources grouped by *f*-number.

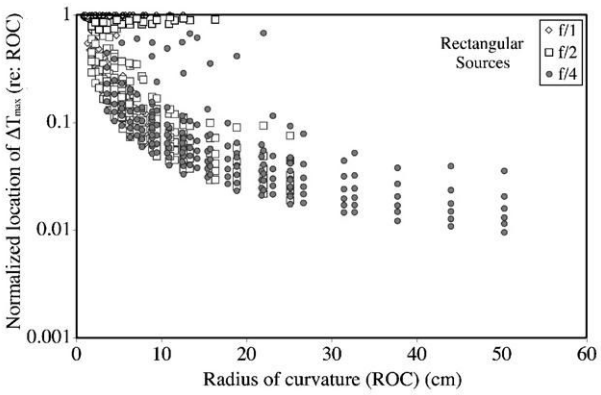

Fig 17.

Paired location of the geometric focus (ROC) vs. normalized location (axial distance) of ΔT_{max} (location of ΔT_{max}/ROC) for rectangular sources grouped by *f*-number.

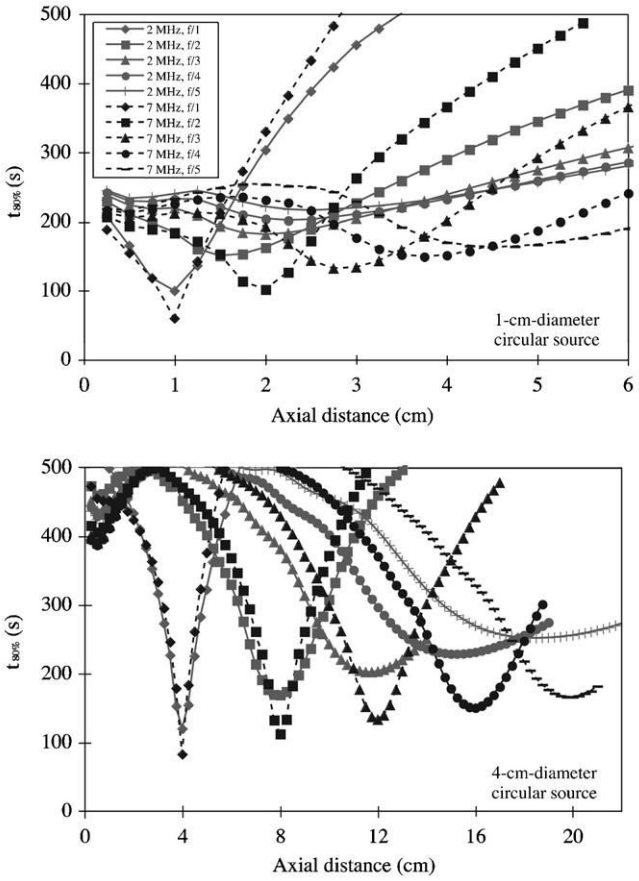

Fig 18.

$t_{80\%}$ profiles as a function of axial distance for the 2-MHz (gray) and 7-MHz (black) cases for circular sources under the condition that the derated (0.3 dB/cm MHz) spatial-peak, temporal-average intensity $I_{SPTA.3}$ is 720 mW/cm^2.

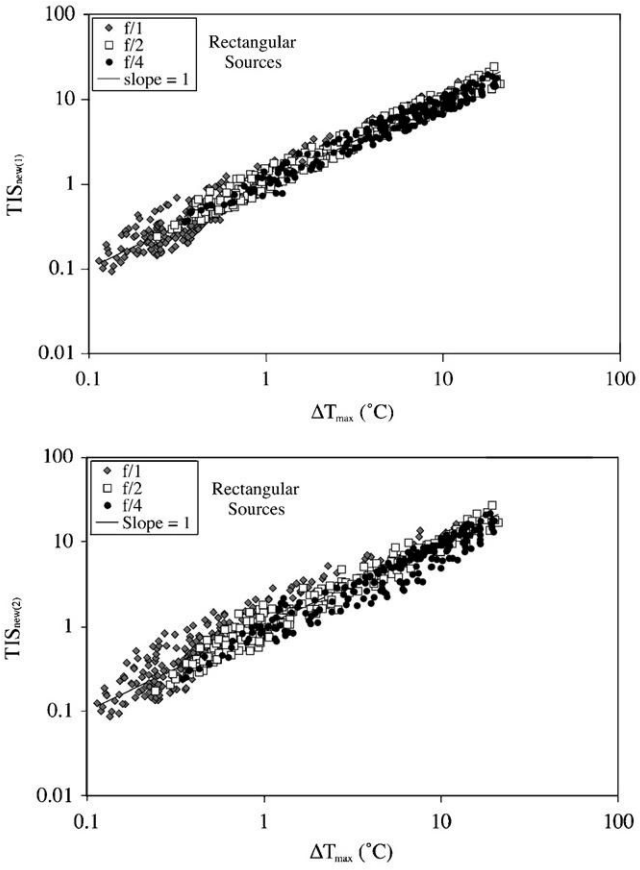

Fig 19.

Paired maximum steady-state temperature increase ΔT_{max} vs. the proposed unscanned-mode soft-tissue Thermal Indices ($TIS_{new(1)}$ and $TIS_{new(2)}$) for rectangular sources grouped by *f*-number under the condition that the derated (0.3 dB/cm MHz) spatial-peak, temporal-average intensity $I_{SPTA.3}$ is 720 mW/cm^2.

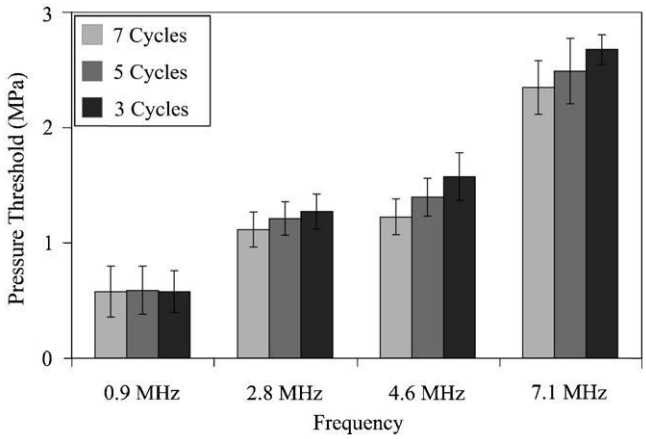

Fig 20.
Peak rarefactional pressure rupture threshold of Optison™ as a function of frequency and pulse duration. PRF = 10 Hz.

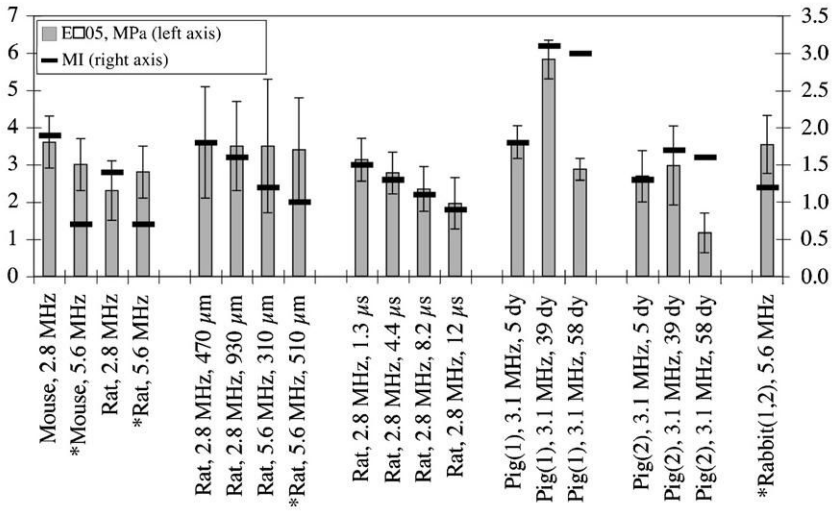

Fig 21.

Summary of ED05 (5%) lesion occurrence thresholds in terms of $p_{r(\text{in situ})}$ (MPa) (bars; left axis) and MI (lines, right axis). *denotes the studies that are evaluated under the same exposure conditions. Error bars are SEMs. These data, by groupings from left to right, are derived, respectively, from Zachary et al. (2001a) and O'Brien et al. (2001,2003a,b,2006).

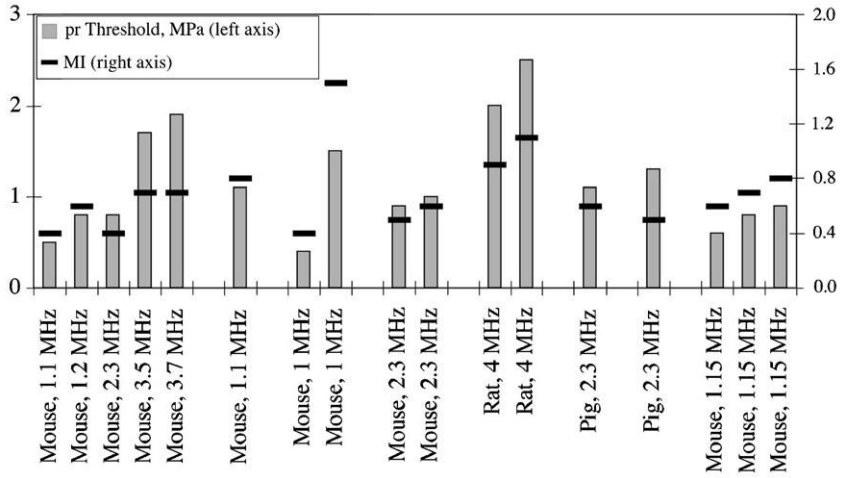

Fig 22.

Summary of lesion occurrence thresholds in terms of $p_{r(\text{in situ})}$ (MPa) (bars; left axis) and MI (lines, right axis) from studies not using our experimental techniques and statistical approach. These data, by groupings from left to right, are estimated, respectively, from Child et al. (1990),Raeman et al. (1993,1996),Frizzell et al. (1994),Holland et al. (1996),Baggs et al. (1996) and Dalecki et al. (1997c,d).

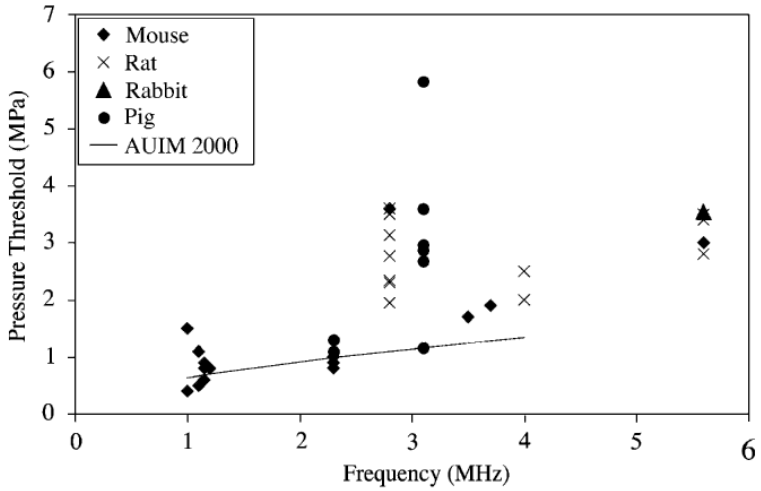

Fig 23.

Global summary of lesion occurrence thresholds in terms of in situ peak rarefactional pressure as a function of frequency for four species (see Figs. 21 and 22). The solid line is the threshold equation derived from pre-2000 data (AIUM, 2000).

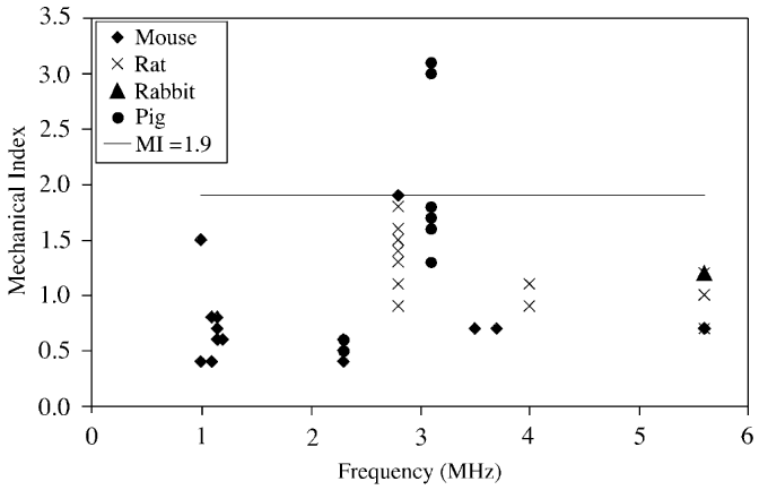

Fig 24.

Global summary of lesion occurrence thresholds in terms of the Mechanical Index as a function of frequency for four species (see Figs. 21 and 22). The solid line denotes an MI of 1.9, the FDA regulatory limit (FDA, 1997).

Table 1

Selected physical properties of pure water at 37 °C

Compressibility (Pa^{-1})	4.4×10^{-10}
Bulk modulus (Pa)	2.3×10^{9}
Density (kg/m^3)	990
Speed (m/s)	1527

Table 2

Typical density, propagation speed and characteristic acoustic impedance values for isotropic media

	ρ (kg/m^3)	***c* (m/s)**	**Z (rayl)**
Gas	1	100–1000	100–1000
Liquid	1000	1000-2000	1–2×10^6
Solid	1000–10,000	2000–10,000 (L) 1500–5000 (S)	10–100×10^6 (L) 4–50×10^6 (S)

L denotes a longitudinal wave and S denotes a shear wave.

Table 3

Typical ultrasonic quantities and units

Quantity	Unit
Charge	Coulomb (C)
Current	Ampere (A = C/s)
Displacement	Meter (m)
Energy	Joule (J = Ws)
Energy density	Joule per meter cubed ($J/m^3 = N/m^2$)
Force	Newton (N)
Frequency	Hertz (Hz)
Intensity	Watt per centimeter squared (W/cm^2)
Length	Meter (m)
Mass	Kilogram (kg)
Power	Watt (W)
Speed	Meter per second (m/s)
Temperature	Degree celsius (°C)
Time	Second (s)
Ultrasonic pressure	Pascal ($Pa = N/m^2$)
Voltage	Volt (V)
Wavelength	Meter (m)

Table 4

List of first-order and second-order quantities used in ultrasound

First-order quantities	Second-order quantities
Current	Energy
Particle acceleration	Energy density
Particle displacement	Intensity
Particle velocity	Power
Ultrasonic pressure	
Voltage	

Table 5

FDA's pre-amendments levels of diagnostic ultrasound devices (FDA, 1985)

	Derated intensity values		
	I_{SPTA} (mW/cm^2)	I_{SPPA} (W/cm^2)	I_m (W/cm^2)
Cardiac	430	65	160
Peripheral vessel	720	65	160
Ophthalmic	17	28	50
Fetal imaging and other[a]	46	65	160

[a] Abdominal, intraoperative, small organ (breast, thyroid, testes), neonatal cephalic, adult cephalic.

Table 6

FDA's pre-amendments levels of diagnostic ultrasound devices (FDA, 1987)

	Derated intensity values		
	I_{SPTA} (mW/cm^2)	I_{SPPA} (W/cm^2)	I_m (W/cm^2)
Cardiac	430	190	310
Peripheral vessel	720	190	310
Ophthalmic	17	28	50
Fetal imaging and other[a]	94	190	310

[a] Abdominal, intraoperative, small organ (breast, thyroid, testes), neonatal cephalic, adult cephalic.

Table 7

AIUM statement on mammalian in vivo biological effects (AIUM, 1988)

(Approved August, 1976. Revised and approved October, 1987)

A review of bioeffects data supports the following statement:

In the low megahertz frequency range there have been (as of this date) no independently confirmed significant biological effects in mammalian tissues exposed in vivo to unfocused ultrasound with intensities[a] below 100mW/cm^2, or to focused[b] ultrasound with intensities below 1W/cm^2. Furthermore, for exposure times[c] greater than one second and less than 500 s for unfocused ultrasound, or 50 s for focused ultrasound such effects have not been demonstrated even at higher intensities, when the product of intensity and exposure time is less than 50 joules/cm^2.

[a] Free-field spatial peak, temporal average (SPTA) for continuous wave exposures, and for pulsed-mode exposures with pulses repeated at frequencies greater than 100 Hz.

[b] Quarter-power (−6 dB) beam width smaller than four wavelengths or 4 mm, whichever is less at the exposure frequency.

[c] Total time including off-time as well as on-time for repeated pulse exposures.

Table 8

t_{43} thermal dose values for various tissues (Lyng et al., 1991;Dewey, 1994).

Tissue	Species	t_{43} (min)
Muscle, fat	Pig	240
Skin	Human, rat, mouse	210
Esophagus	Pig	120
Cartilage	Rat, mouse	120
Breast	Human	100
Bladder	Dog, rabbit	80
Small intestine	Rat, mouse	40
Colon	Pig, rabbit	30
Liver	Dog, rabbit	30
Brain	Cat, dog	25
Kidney	Mouse	20

Table 9

Temperature-time threshold-based data for various biological materials

Fig. 8 symbol	Time (s)	Temp (°C)	Material	Reference
Open triangle	1	69.1	Cat brain in vivo	Lerner et al. (1973)
Open triangle	10	53.4	Cat brain in vivo	Lerner et al. (1973)
Open triangle	100	44.6	Cat brain in vivo	Lerner et al. (1973)
Filled-in circle	1.4	65	Cat brain in vivo	Lele (1977)
Filled-in circle	1.8	64	Cat brain in vivo	Lele (1977)
Filled-in circle	2.5	63	Cat brain in vivo	Lele (1977)
Filled-in circle	3	65	Cat brain in vivo	Lele (1977)
Filled-in triangle	10	53	Rabbit brain in vivo	Vykhodtseva et al. (2000)
Filled-in triangle	30	48	Rabbit brain in vivo	McDannold et al. (2004)
Filled-in triangle	30	47.8	Rabbit brain in vivo	Chen et al. (2002)
Filled-in square	9	60.2	Rat brain in vivo	Pond (1968)
Filled-in square	3	63.7	Rat brain in vivo	Pond (1970)
Open diamond	30	47.2	Rabbit muscle in vivo	McDannold et al. (2000)
Open diamond	30	47.5	Rabbit muscle in vivo	Cheng et al. (2003)
Open circle	180	51	Dog prostate in vivo	Peters et al. (2000)
Open square	1	57	BHK cells in vitro	Borrelli et al. (1990)
Dashed line[a]	0.1	64.5	Multiple tissue thresholds	Lele (1983)
Dashed line[b]	770	41.5	Multiple tissue thresholds	Lele (1983)
Shaded line[a]	60	46.2	Multiple in vitro thresholds	Henle (1983)
Shaded line[b]	840	42.9	Multiple in vitro thresholds	Henle (1983)

[a] Minimum time value is that reported in the article.

[b] Maximum time value was truncated to fit the curve.